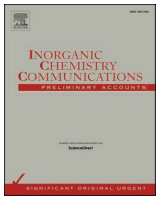
Inorganic Chemistry Communications 181 (2025) 115191



Contents lists available at ScienceDirect

Inorganic Chemistry Communications

journal homepage: www.elsevier.com/locate/inoche





Synergy in metal oxide/metal sulfide binary composites for photocatalysis: mechanisms, applications, and emerging trends

Atiqa Aslam [a], Nimra Nadeem [a], Balaussa Balgabayeva [b,c], Sami Ullah Khan [d], Qamar Abbas [e], Saima Noreen [a], Muhammad Zahid [a,*], Zhazira Supiyeva [b,c,**]

[a] Department of Chemistry, University of Agriculture, Faisalabad 38040, Pakistan
[b] Faculty of Chemistry and Chemical Technology, Al-Farabi Kazakh National University, Almaty, Kazakhstan
[c] Laboratory of Engineering Profile, Satbayev University, Almaty, Kazakhstan
[d] Paracelsus Medical University, Strubergasse 21, 5020 Salzburg, Austria
[e] Faculty of Chemical Technology, Poznan University of Technology, 60965 Poznan, Poland

ARTICLE INFO

Keywords:
Nanohybrids
Synergistic effect
Degradation
Organic pollutants
Advanced oxidation processes
Photocatalysis

ABSTRACT

The uncontrolled release of synthetic toxins and micropollutants from industry and consumer sources into freshwater bodies poses a serious risk to aquatic environments and human health. Advanced oxidation processes, specifically heterogeneous photocatalysis, have drawn attention to solve these issues and a possible route to improve the quality of the aquatic environment. This has been obtained by investigating unique materials that can function synergistically with one another. The scientific society has explored different photocatalyst types. Nevertheless, heterojunction photocatalysts in general and binary heterojunction photocatalysts in particular have demonstrated remarkable qualities and unique advantages. The combined impacts of metal oxides (MOx) and metal sulfides (MS) have a dominant synergistic effect. Therefore, metal oxide/metal sulfide heterojunctions are emerging as revolutionary photocatalysts in environmental solutions. Binary composites such as ZnO/ZnS, CuO/CuS, ZnO/CuS, and many others are discussed for their synergetic photocatalytic efficiencies in the degradation of a variety of pollutants, including insecticides, dyes, pesticides, antibiotics, and heavy metals. This review explores multifaceted roles of MOx/MS highlighting the potential of these heterojunctions as a promising pathway towards a more sustainable future. Further, a detailed understanding is provided on how heterojunctions have been employed to catalyze environmental remediation by investigating their different electrical interactions and catalytic capabilities. Finally, the manuscript will recommend guidelines for further advancement in this rapidly evolving, multidisciplinary field of current interest.

1. Introduction

A clean and safe environment is necessary for the survival of all living things therefore the quality of the environment is a big concern today because environmental pollution has spread all over the world. Some factors that are involved in environmental pollution are globalization [1], economic development [2], trade [3], and industries. Among the various forms of environmental contamination, water pollution is a serious problem for the entire planet. One of the utmost essential resources for all living organisms in the ecosystem is water, which can be contaminated by a wide range of hazardous substances including heavy metals, dyes, medications, pesticides, and herbicides. The harmful effects of these toxic pollutants include gastrointestinal tract disorders [4], respiratory disorders [5], cardiovascular diseases [6], and damage to vital organs like the heart [7], liver [8], kidneys [9], pancreas [10] etc. They are transported through the food chain and bioaccumulation in living species, including plants, animals, and human cells [11]. Almost everything that humans do involves the usage of

Abbreviations: MOx/MS, Metal oxide/Metal sulfides; OPs, Organic Pollutants; TC, Tetracycline; ER, Eosin Red; TB, Trypan blue; QDs, Quantum Dots; MBT, 2-mercaptobenzothiazole; CV, Crystal violet; MO, Methyl orange; TM, Thiamethoxam; RhB, Rhodamine B; PhP, Phenazopyridine; CR, Congo Red; MR, Methyl Red; MB, Methylene Blue; MeB, Methyl Blue; CB, Conduction Band; VB, Valence Band; NCs, Nanocomposites.

* Corresponding author.
** Corresponding author at: Faculty of Chemistry and Chemical Technology, Al-Farabi Kazakh National University, Almaty, Kazakhstan.
E-mail addresses: rmzahid@uaf.edu.pk (M. Zahid), zhazira.supiyeva@kaznu.edu.kz (Z. Supiyeva).

https://doi.org/10.1016/j.inoche.2025.115191
Received 28 May 2025; Received in revised form 21 July 2025; Accepted 25 July 2025
Available online 27 July 2025
1387-7003/© 2025 Elsevier B.V. All rights are reserved, including those for text and data mining, AI training, and similar technologies.

water. But it gets polluted after use and the same water usually goes into rivers, lakes, seas, and other bodies of water that are unsuitable for human consumption. Based on data from the United Nations, it appears that wastewater pollution is a serious problem that affects both advanced and developing nations. Each year, diseases caused by polluted water kill about 297 thousand children, and about 80 % of the water is returned to the environment without treatment [12]. Water should be purified before it can be discharged into the atmosphere to prevent more pollution. So, wastewater treatment can be a hope to disinfect the environment because it can remove pollutants like heavy metals, dyes, antibiotics, and pesticides from polluted water [13].

Many efforts have been conducted to eradicate these toxins from polluted water and there is a lot of interest in treatment of polluted water, particularly in the removal of a variety of organic impurities using environmentally acceptable and economically viable methods [14]. Adsorption, membrane filtration, oxidation, photocatalytic degradation, and UV radiation are a few methods that are frequently used to clean water [15]. Photocatalytic degradation is one of the most commonly used and environment-friendly approaches for water remediation [16]. So, the usage of suitable approaches and materials for the efficient elimination of different pollutants is becoming important [17]. In this context, the practical use of nanoscience and material science for generating energy, disinfection of water, biomedical, sensing, and other applications has solved many disputes of environment, energy, and health. Nanoscience and nanotechnology are interrelated fields that integrates chemistry, physics, and material science [18,19]. Nanocomposites can be defined as those composites whose at least one dimension is less than 100 nm and these are attracting the attention of worldwide scientists because of their multifunctional properties and can be used for treatment of polluted water. Much research has been conducted to fabricate these NCs by different synthesis methods with effective properties like efficiency and stability [20]. A lot of photocatalytic materials containing metal oxides, hydrides, metal sulfides, halides, nitrides, and organic materials have been used for environmental applications.

Among them, metal oxide nanoparticles have been investigated for various uses for instance, devices for storing energy, sensors, environment remediation, and many others [21]. Metal sulfide NCs have an insignificant advantage over metal oxides because of their suitable band gap, greater surface region, and promising photocatalytic activity. The present review will emphasize the synergistic effect of both MOx/MS heterojunctions and their environmental applications. Heterojunctions are created when two individual materials are combined, and because of this combination properties of both materials become enhanced. Compared to pristine semiconductor photocatalysts, heterostructure photocatalysts typically exhibit greater photodegrading proficiency because of improved separation efficiency of electron-hole pairs or inhibiting the electron-hole pairs recombination, resulting in more charge transporters to generate radical species [22]. So, heterostructures are advanced materials with additional properties that can be used for wastewater remediation.

Metal oxides are formed from the coordination of metal ions with oxides, and have a significant role in materials science and many other disciplines. Metal oxide nanoparticles have remarkable physical, optical, electrical, and chemical characteristics [23]. Moreover, the surface atoms of metal oxide nanoparticles (MONPs) are more readily available to participate in reactions than the inside atoms [24]. The well-controlled structural, crystal-like, and surface features of metal oxide-based nanomaterials enable them to serve as wide-bandgap semiconductors. However, narrow bandgap metal oxides such as CuO [25], MnO_2 [26], and Fe_2O_3 [27] are also reported and provide extended light absorption into the visible range. Metal oxide nanoparticles come in various forms of morphologies, which provide varying crystal facets as active sites for adsorption and utilization in photocatalytic processes [28]. They also exhibit favorable properties in water, such as stability and non-toxicity, making them ideal for the degradation of different types of contaminants. Because of these qualities and amazing surface qualities, transition metal oxide nanoparticles are used in environmental remediation processes. The applications of metal oxide NCs depend on many properties, like surface area, size, shape, and photocatalytic properties. When materials are reduced in size from bulk to nanoscale, the surface-to-volume ratio increases, which is favorable for working as a semiconductor photocatalyst [17]. ZnO, CuO, WO_3, TiO_2, SnO_2, Bi_2O_3, Al_2O_3, NiO, iron-based oxides, and other nanosized metal oxides are extensively used in environmental remediation. The main drawback of metal oxide is the higher band gap due to which it only absorbs a small range of visible light. Many methods have been implemented to eradicate these drawbacks, such as doping of different metals, heteroatoms, and the formation of their heterostructures.

Sulfides have recently been reported to be effective in dealing with the aforementioned difficulties. Metal sulfides are semiconductors where the sulfur atom is an anion that forms bonds with cations (monovalent, Ag^{1+}, bivalent cations, e.g., Zn^{2+}, Cd^{2+}, or multivalent, e.g. Fe^{3+} or Mo^{4+}) [29,30]. Transition metal sulfides are a significant category of semiconductor photocatalysts, and they can facilitate redox reactions under milder circumstances. Metal sulfides and their derivatives are sensitive, functional, and environmentally friendly catalysts due to their wide-ranging durability, porous features, great surface region, chemical significance, and affordability. Furthermore, metal sulfides are easily activated under visible light, eliminating the need for other co-catalysts or sensitizers. There is no production of toxic intermediates or byproducts, which means they fully back green chemistry approaches [31]. A slight advantage of metal sulfide-based materials over metal oxides is that the sulfides immediately interact and efficiently use visible light due to their small band gaps. Metal sulfides, like metal oxides, are appropriate for the decontamination of air and water through photocatalysis [32,33].

Metal oxides/metal sulfides heterostructures can be used for the efficient elimination of different toxic pollutants. These have remarkable properties as compared to pristine metal oxide and metal sulfide NCs. When metal oxides and metal sulfides with suitable band gaps are mixed, their photocatalytic properties become enhanced due to the proficient transportation of electron and hole charges and utilization of the maximum part of sunlight [34]. In this way, the production of heterojunctions can overcome some of the disadvantages of bare metal oxides, such as their large bandgap, intense electron-hole pair recombination, and less thermodynamically stable metal sulfides [22]. Because of its potential features, MOx/MS heterostructure has gained significant importance in latest years [35].

This review will cover the details of metal oxide/metal sulfide heterojunctions synthesis, along with the synergistic effect of metal oxide/metal sulfide heterojunctions in their environmental applications. There will also be a thorough discussion of the morphologies of heterostructures and how they impact metal oxide/metal sulfide heterojunctions' photocatalytic performance. The photocatalytic degradation of a variety of organic pollutants such as dyes, herbicides, pesticides, pharmaceuticals, etc., has been discussed and linked with the synergy of the MOx/MS heterostructure. The detailed possible mechanisms of MOx/MS heterojunctions have been discussed to correlate with their respective roles.

2. Heterojunction

A heterojunction is an interaction edge made by the hybridization of two distinct semiconductor photocatalysts with differing band gaps. When a suitable light is irradiated, electron and hole species are produced on the planes of both photocatalysts, and after some time these species again recombine. However, the recombination of these electron–hole pairs is a major issue in photocatalysis. On the other hand, in a heterojunction, semiconductors A and B are mutually used to reduce the losses due to merging. Therefore, in order to overcome these major disadvantages of photocatalysis, heterojunction photocatalysts is used

[36,37]. The representation of heterojunction formation and photocatalysis mechanism is shown in Fig. 1. The creation of heterojunctions is likely to keep electron-hole pairs apart, preventing the coupling of charges. It contributes to the retention of redox reactions at various positions and the maintenance of energy band gaps [38]. Although heterostructures can even create their own problems of interfacial defects, lattice mismatch, or poor band arrangement that can increase the rate of charge recombination and cause lower degradation efficiency [39]. But the most significant advantages of heterojunction photocatalysis include (i) the ability of heterojunctions to absorb light at higher wavelengths. As visible light accounts for 45 % of the solar spectra, the use of semiconductor binary photocatalysts can enhance the utilization of natural light to a broader wavelength region [40]. (ii) Improved separation between electron-hole pairs. In heterojunction photocatalysis, electron and hole pairs travel in the system because of the proper connection of semiconductor materials, which increases the separation efficacy [41]. (iii) Enhanced catalytic activity as a result of integrating another semiconductor [42,43]. Consequently, heterojunctions enhance the availability of more radical species which improve the removal effectiveness of different OPs. Over the past few years, many types of heterojunction photocatalysts have been created and improved. On the basis of separation mechanism of charge carriers, heterojunctions are divided into two classes: The divisions include traditional heterojunctions, these are Type I, Type II, and Type III, and non-traditional heterojunctions include Schottky, p-n heterojunctions, the S-scheme heterojunctions, and the *Z*-scheme heterojunctions.

2.1. Heterojunctions in metal oxide and metal sulfide

Depending on the relative positions of bands and electrical structures of the materials used it can be classified as the straddling heterojunction or Type I, staggered gap or Type II and the broken gap heterojunction or Type III.

2.1.1. Type I heterojunctions

In this heterojunction, the conduction band of semiconductor-A is located at a higher level and the valence band is located at a lower region in comparison to semiconductor-B (Fig. 2a). Thus, under the irradiation of visible light, electrons in the valence band of semiconductor A gain energy and move towards the conduction band. Then, these electrons moved from the conduction band of semiconductor-A towards the conduction band of photocatalyst-B, and the photoinduced holes travel from the valence band of semiconductor-A towards the VB of photocatalyst-B [44]. Type I heterojunction has been described in the synthesis of a β-Ga_2O_3–TiO_2/SiO_2 ternary composite using rice straw as a source of SiO_2 by a mechano-chemical approach [45]. Moreover, there is an example of the creation of a type I heterojunction between two oxides, ZnO and Co_3O_4. As the conduction band potential of ZnO is more negative so the electrons from the CB of ZnO move towards the conduction band of Co_3O_4. It will increase the separation efficiency of electron-hole pairs. These electrons and the holes present in the valence band of ZnO produce reactive radicals, which then degrade various pollutants. In a type-I heterojunction, the CB of photocatalyst-A will lie at a higher level and VB at a lower level than the subsequent semiconductor; thus, the electrons and holes are retained only in the conduction and valence bands of semiconductor B [46]. The accumulation of both charges occurring on the same semiconductor photocatalysts will lead to delayed charge carrier separation and will decrease degrading efficiency [47]. So, another type of heterojunction is required to increase the photocatalytic performance.

2.1.2. Type II heterojunctions

Out of all the conventional types of heterojunction systems, type-II heterojunction has a peculiar misaligned band structure between two semiconductor materials, it is very advantageous in the sense that electron-holes pairs are effectively separated to reduce re- combination rate. Here, semiconductors A and B have closely held comparable band potentials, resulting in a very stable heterostructure [36]. The staggered band system is another name for type II heterojunctions, which are named thus owing to the dissimilar band alignments between the two semiconductor materials. Electrons are transported from photocatalyst A with the greater conduction band to the CB of semiconductor B, while holes are moved from semiconductor B with the lower valence band to the VB of semiconductor A. Electrons and holes travel in opposing ways in a type II heterojunction (Fig. 2b**).** Furthermore, the IEF (Internal electric field) promotes the parting and transportation of charged species. As a result, there is less electron-hole recombination and a greater increase in the electron's lifetime. These ideal band locations in type II heterojunctions can efficiently separate the electron and hole pairs. So, the type II heterojunction is the most favorable for photocatalysis because it allows for the efficient segregation of electron-hole pairs. Significant efforts have been undertaken in the last few decades to

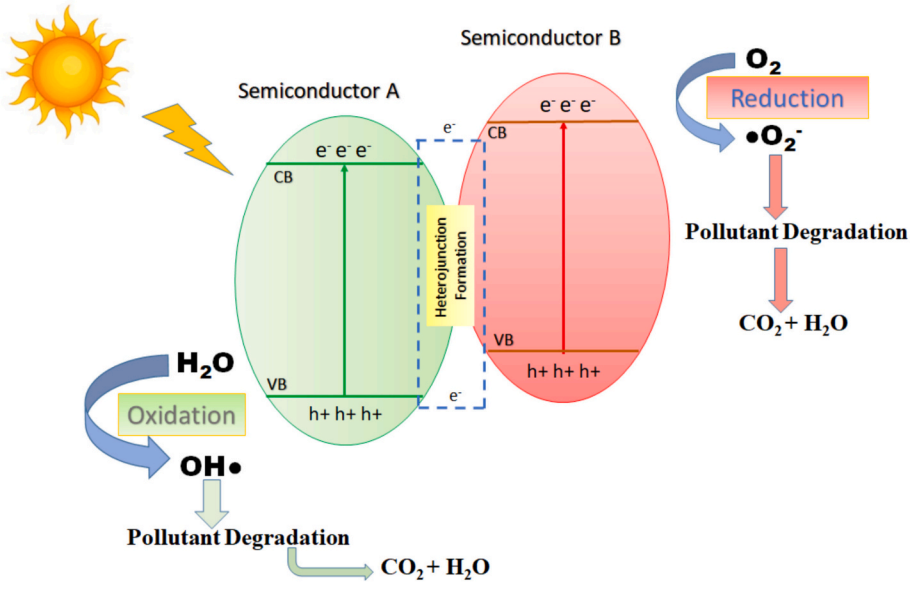


Fig. 1. Representation of photocatalysis on a semiconductor heterojunction.

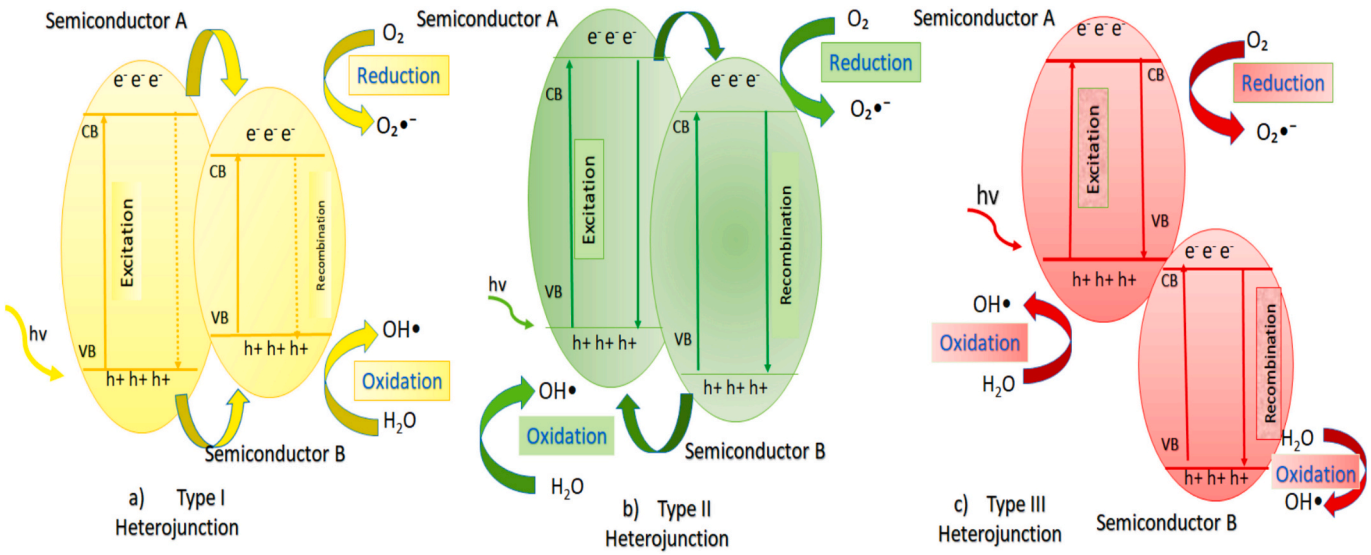


Fig. 2. Representation of band structure and mechanism of charge transfer of traditional heterojunctions a) Type I, b) Type II, and c) Type III.

synthesize various type-II heterojunction photocatalysts, including ZnO/WS_2 [48], ZnO/ZnS [49], ZnO/ZnS/CeO_2 [50], ZnO/CdS [51], and so on for improving the photocatalytic activity. In case of ZnO/ZnS, as the conduction band potential of ZnS is more negative so electrons move from ZnS towards the CB of ZnO and produce the $O_2^{\bullet}$ that degrades MB dye and produces CO_2 and H_2O. The values of h^+_{vb} represent that holes move from VB of the ZnO towards the valence band of ZnS and participate in the reaction of genration of hydroxyl radicals [49]. Despite having a higher electron-hole pair separation ability, there are significant drawbacks of type-II heterojunction photocatalysts that limit their practical usage. One of these drawbacks is the redox reactions taking place on semiconductors with low reduction and oxidation potentials due to which the photocatalyst's redox potential is reduced. Furthermore, the electrons are transferred from the conduction band of photocatalyst A to the CB of photocatalyst B [52], as well as the corresponding transportation of holes from the valence band of semiconductor B to the VB of semiconductor A, are physically critical due to electrostatic repulsion between charged carriers like electron-electron and hole-hole charges [47]. For that reason, the creation of more active heterojunctions in photocatalysis is instantly desired.

2.1.3. *Type III heterojunctions*

The design of type-III heterojunction photocatalyst can be compared to that of the type-II heterojunction, with the exception of that the bandgaps of the type III heterojunction do not overlap due to the extremely staggered gap (Fig. 2c). The misalignment of energy bands results in distinct electrical characteristics, like the creation of quantum wells or confinement effects. These features can be employed in a series of applications, for example photovoltaics, light-emitting diodes (LEDs) and lasers. Consequently, the type-III heterojunction is inadequate for improving the segregation of electron-hole charges because it cannot support electron-hole transportation between the two semiconductors [53]. Among conventional photocatalysts, type-II heterojunction typically has strong efficiency of electron–hole separation, a broad range of light captivation, and quick mass transfer.

2.2. *Non-traditional heterojunctions*

The non-conventional/non-traditional heterojunctions are p-n, Schottky, *Z*-scheme, and S-scheme heterojunctions. The in-depth mechanisms and some instances are described below:

2.2.1. *p-n heterojunctions*

It is believed that this heterojunction is a progressive type-II heterojunction. An additional electric field is introduced to mitigate the limitations of type II heterojunction and this IEF speeds up the flow of electron/hole species and enhances degrading efficiency [36].When light is not irradiated, electrons from the n-type semiconductor transferred into the p-type semiconductor via the p-n junction contact. The n-type semiconductor tends to absorb holes from the p-type photocatalyst at the same time. This process of e^- and h^+ diffusion will keep happening until the system achieves equilibrium at the fermi level. Consequently, at the p–n junction interface, an IEF forms [52]. When these semiconductors are irradiated with incoming light both p-type and n-type photocatalysts can be excited, resulting in the creation of electron-hole pairs. The IEF causes the movement of photoinduced electrons from the p-type photocatalyst towards the conduction band of the n-type semiconductor while at the same time, transfer of holes from the n-type semiconductor towards the VB of the p-type semiconductor also takes place (Fig. 3a). This is the reason for spatially separate electron–hole pairs from one another. It should be prominent that in a p-n heterojunction system, separation procedure of electron-hole pairs is also thermodynamically promising because conduction and valence bands of the p-type photocatalyst are usually at higher level than those of the n-type photocatalyst [47]. As a consequence, the separation efficiency of electron-hole pairs in the p-n heterojunction system is speedier than that of type-I and type-II heterojunctions because of the synergistic effect between the IEF and band configuration. In addition to the p–n heterojunctions, other types of semiconductors such as p–p type, which comprises both p–type, and n–n type, which comprises both n–type semiconductors also exist. Charge separation and migration take place rapidly in p–n type heterojunctions than in p–p type heterojunction and n–n type heterojunction systems [54]. $BiFeO_3/SnS_2$ p-n heterojunctions have been developed for pollutant degradation [55]. Many photocatalysts have been synthesized based on p-n heterojunctions for environmental remediation such as CuO/CdS [56], CuO/ZnS [57], and CuO/CdS [58].

2.2.2. *Schottky heterojunctions*

The Schottky heterojunction is made up of a semiconductor photocatalyst and a metal, which work together to create an efficient space-charge area. On the two-unit interface, electrons are rapidly transported from the semiconductor towards the metal. As a consequence, the Fermi energy levels are aligned, the rate of merging of charge carriers species is reduced, and the efficiency of photocatalysis is boosted [40].

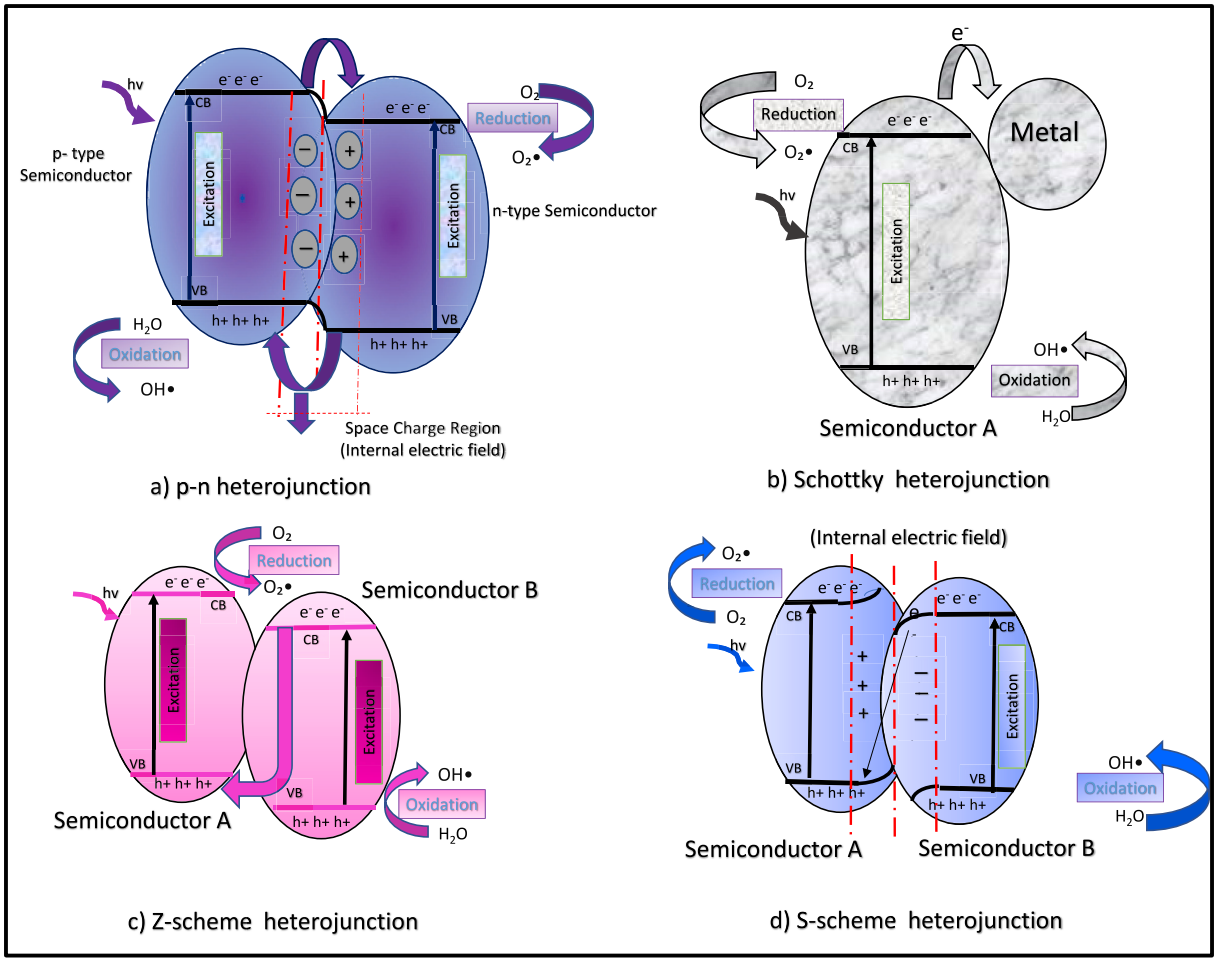


Fig. 3. Band structure of non-traditional heterojunctions. a) p-n Heterojunction system, b) Schottky system, c) *Z*-Scheme Heterojunction system, and d) S-Scheme Heterojunction Photosystem.

In p-type photocatalysts, most of the charge transferors are positive holes, and it will cause to draw electrons from the metal and neutralize the semiconducting photocatalyst material. As a result, n-type semiconductor materials are often used to build Schottky-like barriers [59]. Owing to uneven Fermi energy levels, a Schottky barrier forms, reducing the rate of reunion of electron and hole pairs. When n-type or p-type photocatalysts and cocatalysts form Schottky junctions, the cocatalysts act as charge transporter traps and may assist the speedy transference of photoinduced electrons from the semiconductor to the CB of cocatalysts while photoinduced holes transferred to the valence bands of the cocatalyst. By following this path electrons and holes can successfully be separated (Fig. 3b**)**. Noble metals for example silver (Ag), platinum, palladium (Pd), and gold (Au) are used in composites to improve their photocatalytic performance. The synergistic effect of metal NCs on the surface of the photocatalyst semiconductor improves the separating efficiency of charge transporters [60–62]. Wang and coworkers fabricated 2D/2D ultrathin interfacial schottky Ti_3C_2 Mxene/$SnNb_2O_6$ nanosheets using ultrasonication-assisted hydrothermal procedures [63]. The Au/Pt/SnO_2 ternary composite photocatalyst was found to remove nearly 100 % of 4-nitrophenol in under 8 min. This greater removal efficacy is due to the increased natural light usage by lowering the bandgap of SnO_2 from 3.6 to 3.2 eV after alteration. This composite also shows recyclability and sustainability for up to four successions [64].

2.2.3. *Z-scheme heterojunctions*

This heterojunction has a band placement comparable to the type-II heterojunction however the process of transportation of charges is not the same. In this non-traditional heterojunction system, oxidation happens on the semiconductor's surface with a higher oxidation potential, while reduction occurs with a greater reduction potential. As a consequence, in the *Z*-scheme heterojunction charge transfer occurs owing to the electrostatic pull between electrons and hole species. This transportation mechanism of charges at the Z-scheme heterojunction is easier as related with the traditional heterojunction especially type-II heterojunction [65]. This heterojunction can be categorized into conventional and direct *Z*-scheme heterojunctions. In the conventional Z-scheme heterojunction, a redox facilitator serves as the charge transporter. And it was suggested by Bard in 1979, and it has good redox properties and improves charge separation efficiency. However, the leading shortcomings of this scheme are that it is restricted to the solution phase and is subject to pH sensitivity and undesired side reactions. Whereas on the side of direct *Z*-scheme heterojunction, no intermediary structure is included, this heterojunction is comparable to photosynthesis, with significant electron-hole separation probability and redox capacity [66]. A Z-scheme heterojunction can only be effectively fabricated if the two semiconductor photocatalysts have a appropriate band gap for both oxidation and reduction reactions. Holes have a great oxidation efficacy, while electrons have a high reduction ability, preventing them from recombining and increasing their separation efficiency. The movement of electrons from the conduction band of photocatalyst II to the photoinduced valence bands of photocatalyst I is easier, in the case of the direct *Z*-scheme photocatalysts, because an electrostatic pull exists between the electrons and the holes (Fig. 3c**)** [67]. Some examples of Z-scheme heterojunction photocatalysts are CdS(QDs)/CeO_2 [68], and

CuO/MoS_2 [69].

2.2.4. S-scheme heterojunction

The step scheme is a novel idea that can be used to define the process of photocatalysis in detail. The S-scheme heterojunctions are found between those two n-type photocatalysts that exhibit a staggered band configuration and resemble the type II heterojunction, with the exception of a distinct mechanism of charge movement [70,71]. Effective charge carrier separation can be carried out by creating heterojunctions between the reduced photocatalysts (RP) and the oxidized photocatalysts (OP). Due to the unequal Fermi levels between reduced photocatalysts (RP) and oxidized photocatalysts (OP), an inner electric field is generated at the boundary. Such electric field plays a critical role in the successful separation of the charge carriers and can retain the involvement of strongly redox-active carriers in the reaction effectively [72]. Furthermore, because of the impulsive movement of electrons from photocatalyst A to B through their interface, until their Fermi energy levels are aligned, an electric field is developed from photocatalyst A, which has a larger work function and a reduced Fermi level, to photocatalyst B, which has a comparatively smaller work function and an elevated Fermi level. At the same time, the CB and valence bands of semiconductor A stoop ascendant because of the depletion of electrons, while the bands of semiconductor B bend descendant owing to the accumulation of electrons. As a result, the weak reductive electrons from the CB of semiconductor photocatalyst B will couple with the weak oxidative holes of photocatalyst A due to the incorporated internal electric field, band edge twisting, and coulombic interfaces [54]. The step-scheme suggestion was the first to propose charge carrier transfer via band bending, analogous to how water flows downhill. For example, a TiO_2/CdS S-scheme heterojunction constructed using an electrospinning approach showed exceptional H_2 production activity, which is 35 times superior to that of pristine 1D TiO_2 nanofibers [73]. The boosted photocatalytic performance is owing to a synergistic interaction between the core-shell configuration and the quick transportation of electron-hole pairs in the S-scheme heterojunction, as shown in Fig. 3d. Song et al. described the S-scheme heterojunction between the $CuCo_2O_4$/ZnS, and this heterojunction facilitates the transportation of electrons in the complex system [74]. In one more recent study, Wang reported the creation of an S-type heterojunction between ZnO and $CuInS_2$ that enhances the localized surface plasmon resonance (LSPR) effect. This enhancement enables the effective utilization of infrared light [75]. For the production of H_2O_2, ZnO/1,6-bis(pyrene)-benzodithiophene diones (PBD) composite was used, and it showed the production efficiency up to 4.07 mmol g^{-1} h^{-1}, which was 5.4-fold greater than that of pristine ZnO. This is because of an enormous improvement which has been credited to establishing the S-scheme heterojunction [76]. Hydrothermal and solid-state reaction techniques were used to create TiO_2/MoS_2 coated with g-C_3N_4 photocatalyst for the elimination of 4-nitrophenol [77]. The S-scheme photocatalyst structure eliminates the drawbacks of traditional photocatalytic systems due to the successful separation and migration of charges. The special electronic structure of heterojunctions boosts the photocatalytic activity by increasing the reaction rates [78] and the quantum efficiency. This can overcome the problem of poor light adsorption rates and having high rates of recombination of charges of others traditional heterojunction systems [79].

3. Synthesis of metal oxide/metal sulfide heterojunctions

There are different methods to synthesize the metal oxide/metal sulfide heterojunctions. The synthesis techniques used determine various physical and chemical aspects of metal oxide/metal sulfide nanoparticles, including particle size, crystal appearance, and particle shape. These are prepared by different methods like hydrothermal method, solvothermal method, co-precipitation, sol-gel, chemical vapor deposition, and many others [80]. The methods mentioned above are briefly shown in Fig. 4.

The hydrothermal method is one of the most repeatedly used approaches to synthesize various types of materials like metal oxides [81], metal sulfides, zeolites, semiconductors, and even metal oxide/metal sulfide heterojunctions. The mechanism of the hydrothermal method is very simple precursor materials are dissolved in water under magnetic stirring then this solution is shifted into an autoclave under controlled temperature and pressure [82]. With this, solubility of precursors is changing and this will lead to the formation of tiny particles in aqueous media. Then after cooling, synthesized materials are washed with pure water or other appropriate solvent to remove any undesired products [83]. After this, drying is carried out at a specific temperature to get powdery nanomaterials and to remove any excess moisture. Here are some metal oxides/metal sulfides heterojunctions such as CuO/FeS_2 [84], CuO/MoS_2 [85], ZnO/MoS_2 [86], ZnO/NiS [87], WO_3/CuS [88], WO_3/CdS [82], WO_3/MoS_2 [89] and many others which are synthesized till now by hydrothermal method. One significant benefit of the hydrothermal method is the majority of materials may be dissolved in water by adjusting the pressure and temperature [90]. The solvothermal method is also a powerful technique used to synthesize nanomaterials and it includes any solvent except water. It is used to create nanophases in the presence of different solvents for example, methanol, ethanol, ether, and polyol. Under high pressure and temperature, NCs with unique properties are obtained by this method [91]. Co-precipitation is a facile method to prepare nanoparticles in chemistry as well as in other fields of science. The general mechanism of this method is the precipitation of two or more substances or materials from the solution. A chemical reaction occurs between the precursor solution and the precipitating agent. It involves the formation of solid particles, which are our desired products. After this, washing, centrifugation, and drying are the processes, that are required to complete this process. For example, ZnO/CdS nanocomposites were synthesized using chemical co-precipitation in which the appropriate quantity of freshly prepared zinc oxide nanoparticles and cadmium acetate dihydrate was dispersed efficiently in ethanol (50 mL) and followed by the addition of thiourea in the dispersion with continuous stirring. It was performed at room temperature. High-intensity ultrasound irradiation for 2 h was used to formulate ZnO/CdS binary composite. The yellow precipitate was formed, and then these precipitates were centrifuged and thoroughly washed several times with deionized water, followed by successive washings with ethanol, and lastly dried at 70 °C in air to attain the fine powder [92]. Thereafter, this powder was annealed at 200 °C to eliminate unwanted impurities. There are so many other heterojunctions, such as CuO/ZnS [57], ZnO/CuS [93], ZnO/TiS [94], WO_3/ZnS [95], and TiO_2/CuS [96] that are synthesized by the co-precipitation method.

Sol-gel method is a solution-based process through which a wide range of metal oxides/metal sulfides heterojunctions with tailored properties are prepared. These properties are high surface area for nanocatalysts, mechanical strength, electrical conductivity, and control over the size and shape of heterojunctions [97]. Firstly, sol is formed in this method, and sol contains precursors that react and form the desired product. Then, the process of gelation occurs in which particles become immobilized within a liquid medium. After that, aging and drying processes occur to enhance the properties of the material. In the end, calcination, which is a high-temperature treatment is carried out to remove residual compounds. ZnO/Ag_2S was produced through the sol-gel technique. Equal amounts of zinc nitrate hexahydrate and anhydrous oxalic acid were prepared in deionized water and boiled, and zinc nitrate solution was added swiftly to the oxalic acid. It forms the zinc oxalate (sol 1). A quantity of $AgNO_3$ solution of 5 mL was added to the solution of Na_2S. The sol 1, which contained an amount of zinc oxalate, was added to the formed Ag_2S (sol 2). The mixture was frequently stirred as it cooled down to room temperature. The mixture of the zinc oxalate dihydrate crystals and the Ag_2S was washed multiple times with distilled water, dried under air overnight, and dried at 100 °C for 3 h. Then, powder was heated in the muffle furnace at a temperature of 400 °C



Fig. 4. Overview of synthesis methods for heterojunction structures.

[98]. The ball milling technique has also been used in the preparation of different types of metal oxides/metal sulfides, and it is done through two steps. The first action involved complete compounding of the raw materials, and the second is to refine the particle size of powders [99]. Ye et al. synthesized CdS/TiO_2 binary heterostructure by using the ball milling technique. TiO_2 and CdS powders were measured precisely and poured into the corundum ball mill tanks. Then, these powders were dry-milled with ball milling, which is based on the designed speed (ball milling). Anhydrous ethanol was then mixed to cause the combined materials to exhibit a sticky form, and subjected to the ball mill again under the same milling conditions to be wet ball milled for 2 h. After it, the products were immediately collected, dried, and subjected to a resistance furnace where they were calcined under the conditions of 400 °C [100]. Another synthesis technique, electrospinning, has been used for the preparation of ZnO/CdS nanofibers. Cadmium Chloride $CdCl_2$ was added to ethylene glycol and stirred continuously at 70–80 °C. Drop-wise quantities of thiourea previously dissolved in ethylene glycol were added to the solution of Cd ions. The pure ZnO nanofibers samples were placed in Cd solution; the temperature was raised to 100 °C and held steady at that for a period of 2.5 h. Then the samples were washed using ethanol and water [101]. Ilyas et al. used a pulsed laser ablation in liquid (PLAL) setup for the synthesis of TiO_2/CdS binary heterostructure. The different percentages of the nanoparticles (TiO_2 and CdS) mixture were prepared, sonicated, and positioned on a PLAL apparatus. In the course of the synthesis process, the neodymium-doped yttrium aluminum garnet laser (wavelength = 532 nm) was maintained at the laser energy of 350 mJ/pulse; laser pulse duration 8 ns and laser pulse frequency of 10 Hz within the 45 min period [102].

4. Copper oxide/metal sulfide heterojunctions and their environmental applications

4.1. CuO/CuS heterojunctions

CuO is a p-type semiconductor photocatalyst has band gap of 1.2 to 1.8 eV which makes it suitable for light absorption. Therefore it has shown increased photocatalytic activity and has promising uses in environmental applications [103]. The corrosive nature of semiconductors, on the other hand, may limit catalytic performance [104]. The conduction band of CuS has a higher potential than CuO, so electrons will move from the CB of CuS to the CB of CuO. On the other side, CuO has a higher negative potential valence band than CuS, therefore photoinduced holes will transport from valence band of CuO to the VB of CuS. Nowadays, the most commonly explored technique for improving degrading activity is coupling with additional materials to produce heterojunction photocatalysts [105]. They not only allow for a wide spectrum of light absorption, but they also provide charge separation by segregating electrons and holes into distinct semiconductors [47]. CuO/CuS heterojunctions can lead to effective charge separation. Yuan-Tse Kao [106] and coworkers developed CuO/CuS nanowires for environmental applications. These core-shell nanowires could help to separate electron-hole pairs and improve photodegrading efficiency when irradiated with natural light. This parting of the electron-hole pair may restrict the coupling of the electron-hole pair and be involved in redox reactions, facilitating the elimination of different impurities from the environment. These nanowires show 89 % removal of MB under illumination, which helps to assess the photodegradation efficiency of CuO/CuS heterojunctions. CuO/CuS core-shell nanowires were found to be a hopeful photocatalyst for the degradation of different toxins in poisoned water [106]. CuO/CuS core-shell nanowires have also been used to remove the rhodamine B dye. In this work, it has been demonstrated that RhB can be degraded up to 61 % by employing CuO/CuS photocatalyst [107].

4.2. CuO/group 12 metal sulfides heterojunctions

The synergistic effect of CuO with metal sulfides of Group 12 has also been studied. CuO coupling can significantly improve ZnS photocatalytic efficiency under visible light. CuO, as a p-type photocatalyst with a tapered band gap, may create n-type ZnS active in natural light and facilitate the segregation of electron and hole species by forming a p-CuO/n-ZnS heterojunction. Furthermore, when CuO/ZnS photocatalysts are formed, photoinduced electrons in the CB of CuO are easily shifted to the CB of ZnS, and h^+ in the VB of ZnS are transferred from VB to the of CuO, which is promising for segregating electron-hole pairs to improve photocatalytic efficiency. CuO/ZnS heterojunctions were created by a simple and efficient co-precipitation process and their photocatalytic abilities for dye degradation were investigated. This heterostructure had the highest photocatalytic efficiencies, with degradation rates for MB, MO, and MR dyes of 98.3 %, 94.2 %, and 92.8 %, respectively (Fig. 5a,b) [57]. Cadmium sulfide CdS is desirable for photocatalytic applications have a bandgap of ~2.24 eV. Successive ionic layer adsorption and reaction (SILAR) and thermal oxidation were used to create CuO/CdS composites. Adding CdS to a CuO nanowire's surface will likely enhance the material's photocatalytic capabilities because the surface area of CuO nanowires has increased, which promotes its efficiency. Its

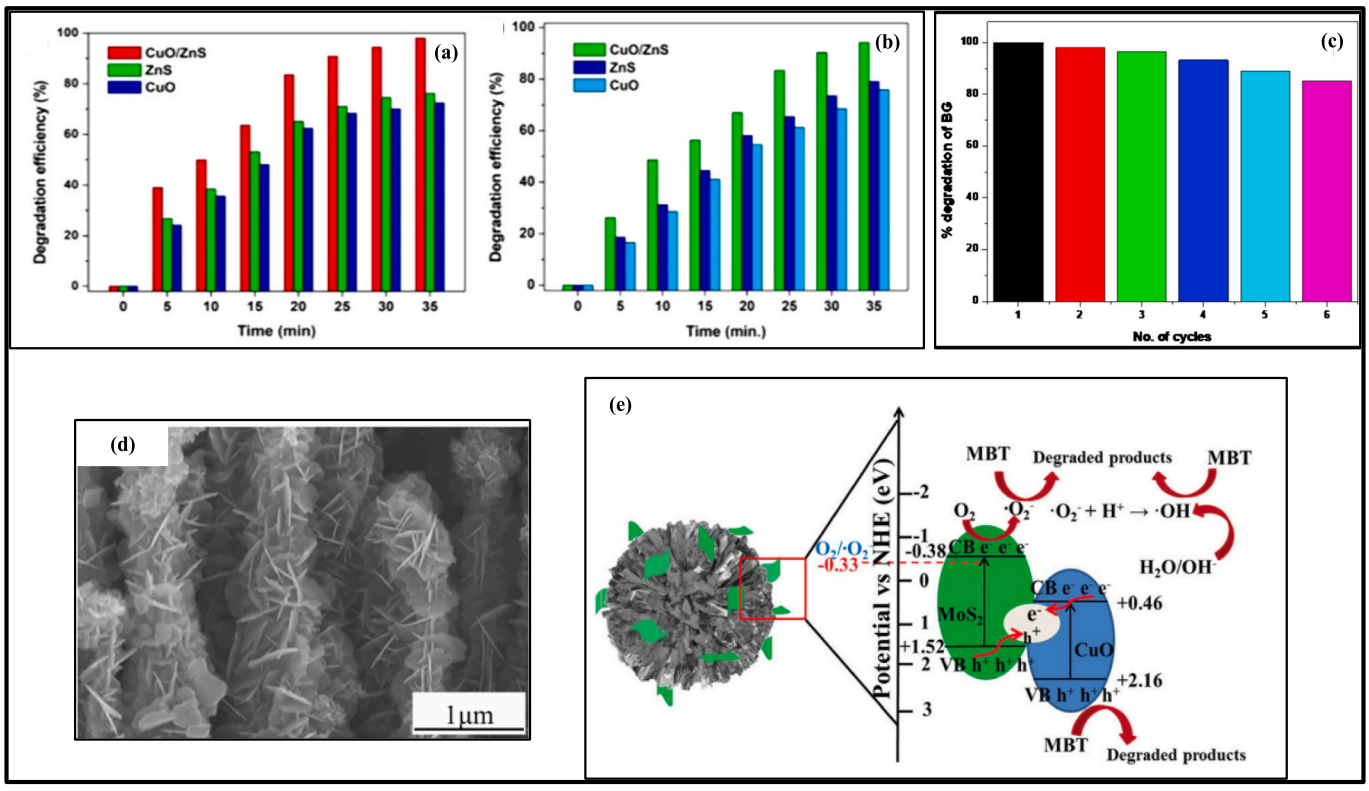


Fig. 5. (a, b) Photocatalytic performance of CuO, ZnS, and CuO/ZnS heterojunction for removal of different dyes [57] (c) FESEM appearance of CuO/CdS [108] (d) Sustainability and recyclability of CuO/FeS_2 Heterojunction [84] (e) Mechanism of *Z*-Scheme heterojunction of CuO/MoS_2 [69].

morphology is shown in Fig. 5d. Illumination with UV and sunlight for 150 min resulted in the highest degradation rate (94 %) of MB [108]. Another work reported CuO/CdS heterojunctions with increased photocatalytic effectiveness due to improved separation and transportation of e/h + pairs. Under natural light exposure, the photocatalytic removal efficacies of CuO/CdS heterostructures were examined for diverse dyes, for example, RhB, MLB, MB, and MO. The obtained degradation proficiencies are 93 %, 75 %, 83 %, and 80 % respectively [58].

4.3. *CuO/other transition metal sulfides*

Heterojunctions of CuO with other transition metal sulfides have also great importance. CuO may be ideal for constructing a *Z*-scheme heterojunction with MoS_2. The fundamental purpose is that the equivalent band gap between CuO and MoS_2 can form an excellent Z-scheme heterojunction, which greatly facilitates charge carrier separation and transportation (Fig. 5e). The other reason is that CuO with a small gap has a high light-gathering capability in the wavelength range, allowing it to make the finest usage of solar energy [109]. The CuO/MoS_2 heterostructure is also favorable to increasing the surface area, resulting in a large number of active sites. Fabricating a heterojunction of CuO with MoS_2 can successfully enhance the degrading efficacy. Therefore, it is substantial to manufacture CuO/MoS_2 heterojunction photocatalyst for efficient degradation of different polluting agents from contaminated water with outstanding activity. The photocatalytic efficiency of CuO/MoS_2 is 95.3 % for RhB and 99.8 % for methyl violet dyes [85]. 2-mercaptobenzothiazole (MBT) is a chemical used in the synthesis of rubber, and it is highly toxic and causes skin diseases. The *Z*-scheme CuO/MoS_2 nanocomposite is the most powerful photocatalyst, with a separation efficiency of photogenerated carriers that is roughly three times that of pristine CuO and five times that of the bare MoS_2. Some researchers also reported successfully generating CuO/MoS_2 Z-scheme photocatalyst with outstanding efficiency (96 %) in the removal of MBT under illumination [69].

In the group of metal sulfides, iron sulfides (FeS) are more significant photocatalysts for the solar-driven reactions owing to their lower bandgap, favorable redox potentials, and non-toxicity [110]. Brilliant green dye is a cationic dye that causes eye and skin irritation, diarrhea, abdominal pain, nausea, and vomiting. The exclusion of BG dye from the unhygienic water is required owing to the tremendous value of dye removal [111]. In response, AOP is the ideal approach for efficiently removing impurities by employing semiconductor materials [112]. CuO/FeS_2 composite was experienced for the photodegradation process in the decontamination of BG dye solution by exposing it to visible light. This heterojunction CuO/FeS_2 proved to be effective for complete dye degradation in 90 min. Furthermore, this binary compound is a stable catalyst that may be utilized for six consecutive cycles with insignificant degradation rate loss (Fig. 5c). It was also verified by XRD analysis because when a reused composite is subjected to XRD, it appears as a fresh composite. Therefore, CuO/FeS_2 composite can be employed to clean polluted water on an immense scale more efficiently and cost-effectively [84].

From all the information above, it has been concluded that CuO is a p-type semiconductor with a lower band gap that can participate in natural light photocatalysis. Still, its efficiencies can be increased by adding other metal sulfide heterojunctions some of which are UV light active. After forming a heterojunction with CuO it can easily perform photocatalysis under visible light instead of UV light. Moreover as compared to traditional heterojunction, non-traditional Z scheme heterojunction of CuO/MoS_2 provides overall efficient results. The morphology of CuO/CuS and CuO/CdS also affects its degradation efficiencies. If we look at CuO/FeS_2 which is more sustainable and recyclable there is only a fraction of a decrease in its degradation efficiency after using it for up to six cycles.

5. Zinc oxide/metal sulfide heterojunctions and their environmental applications

5.1. ZnO/ZnS heterojunctions

Transition metals have key importance in the remediation of environmental pollution especially in photocatalysis. Zinc has been widely used in many heterojunctions for the hydrolysis of water and its oxide i. e. ZnO also has an effective role in the disintegration of environmental pollutants [113]. But ZnO has a quite low degradation productivity [114] as a photocatalyst, owing to its broadband gap and fast coupling of photoinduced electron-hole pairs species, along with the photo corrosion phenomena, which might affect the degrading effect of polluting agents [115]. Many attempts have been made to increase the photooxidation capabilities of ZnO by doping [116], loading with noble metals [117], or adding other semiconductor nanoparticles [118]. However, ZnS nanostructures are naturally favorable because of their large surface space and low density [119]. So, these semiconductors can be used as a potential catalyst for the deterioration of different polluting agents from polluted water. The morphology of ZnO/ZnS heterostructures is hollow nanorods (NRs), which provide a large surface region for photocatalysis (Fig. 6a). Thus, ZnO/ZnS gives 96 % removal efficiency of MB dye under visible light exposure. The conduction band potentials of ZnO and ZnS are −0.31 eV and − 1.94 eV, respectively, and the valence band potential of ZnO is +2.89 eV and of ZnS is +2.56 eV [49]. With another morphology, ZnO/ZnS core-shell nanowires have been made by solvothermal and hydrothermal methods. ZnO and ZnS have close bandgaps with each other, but when ZnS is incorporated into ZnO, their properties become enhanced, for example, less recombination rate of electron-hole pairs, efficient transfer of these carriers, and higher degradation efficiencies. Due to incorporation, a stable heterostructure ZnO/ZnS has formed, so it shows only a small change in efficiency from 98.5 % to 94.4 % up to 10 cycles (Fig. 6b). This heterostructure has also been used to degrade the MB and RhB and showed removal of these dyes up to 98.5 % and 87.5 % respectively [120]. The photocatalytic efficiency of semiconductors depends on many factors, such as morphology and manufacturing methods. ZnO/ZnS heterostructure has also been synthesized by a low-heat solid-state chemical method, which remarkably increases its degradation efficiencies for different dyes. When ZnO is added to ZnS then it changes the band energy structure of ZnS and increases the redox ability because ZnO has strong oxidizing and reducing ability [121]. Due to this, the ZnO/ZnS heterostructure has degradation efficiencies of 96 %, 94 %, and 93 % for methyl orange, RhB, and TC respectively [122]. In a recent study, ZnO/ZnS is synthesized by the biosynthesis method and its efficiency is determined by the degradation of MB dye and antimicrobial activity [123]. Furthermore, this binary composite ZnO/ZnS has been tested by adsorption and photocatalysis processes. The spherical-shaped composites 95.3 % degradation efficiency against MB dye by photocatalysis [124]

5.2. ZnO/coinage metal sulfides heterojunctions

Zinc oxide has recently gained considerable attention among metal oxide nanoparticles [125]. Phenol is used as a raw material in many industrial sectors and it is the source of contamination of industrial wastewater. Congo red dye also contaminates water so to remove these harmful materials researchers worked on the heterojunctions which can easily degrade these materials. In the group of coinage metals, copper has great importance in environmental applications due to its unique properties. On the other side among metal chalcogenides copper sulfide (CuS) is a popular photocatalyst and has also sparked considerable interest in wastewater treatment, water splitting, and the degradation of contaminants from aqueous solutions [126]. ZnO had a large band gap of about 3.2 eV [127] which forms it effective under UV radiation whereas CuS had a narrow band gap between the range of 1.6–2.4 eV and can efficiently work under visible light [128]. So, an efficient

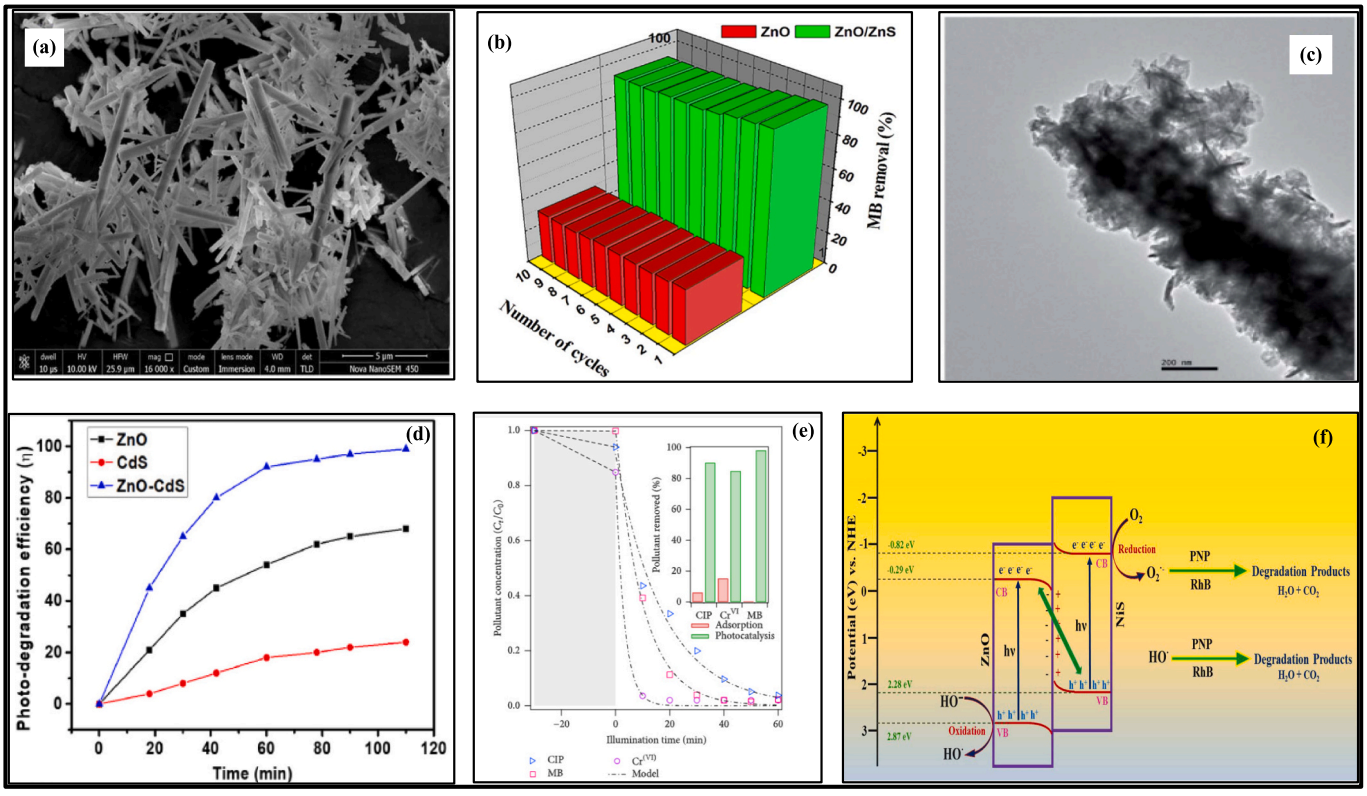


Fig. 6. a) FESEM image of ZnO/ZnS hollow Nanorods [49] b) Reusability of ZnO/ZnS heterojunction [120] c) TEM image of ZnO/CuS Heterostructure [93] d) Photodegradation efficacy of ZnO/CdS heterojunction for deterioration of MB dye [92] e) Photocatalytic degradation of Cr (VI), CIP, and MB over ZnO/SnS_2 [137] f) Possible Mechanism of Photocatalysis [87].

catalyst can be generated by synthesizing a type II heterojunction between ZnO and CuS. Electrons can easily move from CuS towards the ZnO and can produce superoxide radicals which degrade many pollutants. It was found that ZnO/CuS heterojunction improves the photocatalytic elimination of CR and phenol OPs up to 82 % and the morphology of the photocatalyst also affects its degradation efficiency. The hierarchal morphology of ZnO/CuS can be described as CuS is not integrated into the lattice of ZnO nanorods but it only deposits on the surface of ZnO **(**Fig. 6c**)** due to this, it facilitates the process of degradation [129]. MB does not degrade without a catalyst under visible light irradiation so to degrade dye ZnO/CuS heterojunction is used as a catalyst. In another approach ZnO/CuS photocatalyst has been created by the wet chemical method. The morphology of zinc oxide is nanotubes so when it is decorated with CuS it increases the absorption of visible light. It was revealed that type II heterojunction is formed between ZnO and CuS because of this it exhibited a greater visible-light photocatalytic efficiency (87 %) in MB removal [93]. In the metal chalcogenides group, Ag_2S has been researched for a variety of applications, containing photovoltaic cells, photoconductors, and reactive films in optoelectronic devices and infrared detectors. Ag_2S is also used as a semiconductor because of its low band gap of about 1.0 eV and has captivation ability of a wide-ranging solar spectrum. So, ZnO can make an efficient heterojunction with silver sulfide. Therefore ZnO/Ag_2S heterojunction has been used as a photocatalyst in the removal of dyes as compared to bare ZnO and Ag_2S. So it exhibits the acid black 1 dye degradation efficiency of 84.5 % [98].

5.3. ZnO/other transition metal sulfide heterojunctions

Pristine CdS affects human health but its effects are successfully replaced when it is combined with ZnO and form heterojunctions which are used to treat wastewater. The wet chemical method is used to synthesize flower-like ZnO/CdS heterojunctions. Pristine CdS affects human health but its effects are successfully replaced when it is combined with ZnO and form heterojunctions which are used to treat wastewater. In photocatalysis, electrons are moved from CdS to ZnO, and holes are transported in the reverse direction so these electrons and holes react with H_2O molecules and generate radicle species which degrade contaminants. The band alignment in the ZnO/CdS heterojunction results in separation of the electron-hole charges and reducing reunion rate. When ZnO/CdS heterojunctions are utilized for the photocatalytic breakdown of water is improved. These flower-like composites degraded RhB up to 90 % at pH 10 [130]. ZnO/CdS heterojunctions are synthesized by different methods such as hydrothermal synthesis, colloidal synthesis, etc. [131,132], and in all these methods molar ratios of ZnO and CdS are taken differently such as 75:25 and 25:75 [132]. Aqueous chemical growing method has also been used for the synthesizing of ZnO/CdS composite nanorods.3, 4-dihydroxy benzoic acid (DHBA) was effectively deteriorated using ZnO/CdS heterojunction as a photocatalyst when out to visible light [133]. Now, ZnO/CdS NCs have been prepared with equal molar ratios of both components by a superficial co-precipitation method. The degradation proficiency of the heterojunction is investigated by studying the removal rate of (MeB) dye, which is approximately 99 % in 110 min, which is much faster than individual ZnO and CdS semiconductors as shown in Fig. 6d [92]. As reported by the recent research, ZnO/CdS heterojunction shows 90.5 % efficiency in the degradation of MB dye [124]

Among chalcogenides, titanium sulfide can also be used as a semiconductor under UV irradiation so the heterojunctions generated by ZnO and TiS provide an IEF (internal electric field) that improves the segregation of electron and hole pair and induces faster carrier movement. In industrial water effluents and numerous manufacturing industries applications, the ZnO/TiS nanocomposite material was found to be stable and recyclable and they frequently boosted photocatalytic reactions. The photocatalytic efficiency of ZnO/TiS material was assessed on Trypan Blue (TB) dye when exposed to UV light and this composite degraded TB under different conditions like concentration of catalyst, different pH, and amount of dye etc. This heterojunction had also a greater antibacterial activity for medical use [94]. Zinc oxide has a higher band gap so to form its heterojunction a material which has nearly 1.0 eV band gap can be used. In transition metal dichalcogenides (TMDC), MoS_2 has great importance in photocatalysis. Molybdenum disulfide (MoS_2), a semiconductor material, has been regarded as an encouraging natural light active photocatalyst owing to its most stable layered form and absorption in the higher visible region of the solar range [134]. A synergistic interaction between ZnO and MoS_2 is identified, which separates electron-hole pairs and helps to delay the process of recombination hence increasing degrading efficiency. It was shown that the flower-like ZnO/MoS_2 heterojunctions (FZMH) exhibit the highest MB degradation efficacy of 67 % at time 2 h as compared to other dichalcogenides heterojunctions. FZMH also displayed 64, 69, and 84 % antimicrobial activity against *Escherichia coli*, *Pseudomonas aeruginosa*, and *Bacillus subtilis*, respectively [86].

FeS_2 is a semiconductor with photocatalytic properties i.e. low band gap and stability and many hybrid composites are formed with this semiconductor [135]. Zinc oxide can form heterojunctions with FeS_2 due to their band edge alignment and their suitable properties. Therefore, ZnO/FeS_2 NCs were created with different ratios, and their progress in the deterioration of dyes under UV light has been examined. The ZnO/FeS_2 NCs were reported to have the highest MG degradation efficiency (98.0 %) under 40 min of UV exposure. So, this heterojunction shows higher photocatalytic efficiency as compared to bare ZnO [66,136]. Ciprofloxacin (CIP) is an antibiotic that contaminates water and is a source of water pollution. Therefore, it is a need of time to synthesize such heterostructure which can overcome this source of pollution. So, the ZnO/SnS_2 photocatalyst was prepared with a microwave-assisted method to degrade the antibiotic because these two materials have high degrading efficiency as compared to individual ZnO and SnS_2. This heterostructure has other advantages such as it also has been implied to disintegrate other OPs like methylene blue and hexavalent chromium ions. Coating a small quantity of SnS_2 on ZnO results in a significant boost of CIP, methylene blue, and Chromium ion reduction up to 90.2 %, 98.2 %, and 80.2 % respectively **(**Fig. 6e**).** It has been proved that ZnO/SnS_2 heterojunctions are brand-new kinds of visible-light active photocatalysts for environmental applications [137,138].

There are a lot of pollutants that affect our environment and are a serious threat to human beings' lives. Among all these pollutants, dyes and phenolic derivatives are more toxic to human health, so to overcome this problem, a lot of research and environment-friendly technologies have been used. A large number of semiconductor photocatalysts have been used to degrade OPs, for example, ZnO/NiS nanocomposite was used as a photocatalyst to eliminate RhB and p-nitrophenol (PNP) for the first time. NiS can be used as a photocatalyst because of its remarkable properties, it can increase degradation efficiency and also provide a more active region for the process of photocatalysis [139]. The calculated CB of ZnO and NiS were aligned at −0.29 and − 0.82 eV respectively; however, the VB of ZnO was at 2.87 eV, and the VB of NiS was 2.28 eV. This ZnO/NiS forms an S-scheme heterojunction and effectively works under UV radiation because of the band gap of both components **(**Fig. 6f**).** Therefore, photocatalytic degradation of p-nitrophenolate and RhB in UV-light exposure was used to observe the ZnO/NiS heterojunction activity. This photocatalyst removes up to 96 % of p-nitrophenol and 93 % of RhB, which shows higher efficiency as compared to two separate materials [87].

With the above-mentioned information, we concluded that ZnO is an n-type semiconductor photocatalyst with a large band gap value of about 3.6 eV, which proves that it is a UV active catalyst, and forming a heterojunction with other sulfides like CdS makes it functional under visible light. The limitation of CdS is its toxicity and its poor band edges, but these can be mitigated by ZnO, which facilitates redox reactions for the degradation process. In the case of ZnO/CuS p-n heterojunction is

formed between two semiconductors, which assists the separation of e^- and h^+ carriers. Further, CuS is not incorporated into the ZnO nanorods but is only present on their surface, which provides a high surface region and is a reason for higher degradation efficiency. ZnO/NiS has been first time used in water treatment and shows excellent efficiency against pollutants. ZnO/ZnS hollow nanorods provide many catalytic sites for the process of degradation. ZnO/ZnS heterostructure is formed by the incorporation of ZnS into ZnO, and a stable composite is formed.

6. Tungsten oxide/metal sulfide heterojunctions and their environmental applications

6.1. WO_3/group 12 metal sulfide heterojunctions

Among metal oxides, tungsten oxides (WO_3) have been extensively used in environmental applications owing to their distinctive properties such as band gap, its stability and they may be activated in visible light [140]. On the other side metals of group 12 also have been proven efficient photocatalysts in previous studies such as ZnS is a reduction photosystem and can produce photogenerated carriers which are commonly utilized in photocatalysis, H_2 generation, and CO_2 photoreduction [141]. However, ZnS is unstable and self-oxidizes [142], but WO_3 is a stable photocatalyst and has been identified as an oxidation photosystem [143] due to its strong positive potential of the valence band edge. As a result, these two semiconductors can be coupled to form a *Z*-scheme heterostructure, and the mechanism of movement of charges can be modified to improve photocatalytic performance. The incorporation of WO_3 into ZnS boosts visible-light captivation and separation efficiency of electron and hole pairs. Under UV–Vis light, the photocatalytic performance of the linked catalysts and single semiconductors was investigated in the deterioration of tetracycline hydrochloride (TCH) (Fig. 7a**).** TCH is an antibiotic that has great usage in the treatment of diseases. It has been observed that by using WO_3/ZnS heterojunction there was complete degradation of TCH under 90 min which shows that heterostructure highly influences the rate of degradation and presents remarkable degradation efficiency semiconductors which is 50 times more than individual semiconductors (6 % for WO_3 and 14 % for ZnS) [144]. The WO_3/ZnS composite also offers a lot of applications in the treatment of Uranium-containing wastewater because Uranium is a heavy metal which is a serious problem for the aquatic environment. With time Uranium-containing waste material is increasing day by day [145]. To mitigate this problem, there is a need to reduce Uranium U (VI) into U (IV) because U (IV) is not hazardous for living organisms [146]. For this purpose, different heterojunctions have been used in the past for the removal of U (VI) under illumination [147]. The bandgap of ZnS can be reduced by forming a heterojunction with WO_3 and they will easily reduce U (VI) to U (IV) due to their reduction potential [95]. The precipitation process was then used to create WO_3/ZnS composites. The photodegradation performance of prepared materials for U (VI) reduction under illumination was investigated. Almost 93.4 % of Uranium has been reduced by using WO_3/ZnS heterojunction [95].

Cadmium sulfide (CdS) possesses such properties which make it suitable for synthesizing heterojunction with WO_3 such as a wide light range, a high reduction capacity, an energy band structure, etc. [148]. The hydrothermal process was used to synthesize the WO_3 and the precipitation process was used to synthesize WO_3/CdS heterojunctions. Many pollutants contaminate the environment, clean water, and aquatic environment and one of those pollutants is pesticides which are emerging pollutants nowadays. Imidacloprid is one of these pesticides and has a lot of usage in daily life [149]. The photocatalytic degradation performance of WO_3/CdS heterojunction was examined using Imidacloprid (IMD) pesticide degradation under visible light irradiation. Heterojunction shows almost 80 % degradation efficiency which is higher than compared to individual WO_3 and CdS composites. This efficiency was somewhat due to the morphology of WO_3/CdS which offers a high surface region for reaction. The nanowires of WO_3 in the midpoint look like the central part of a flower and adjacent nanorods are petals in which CdS can easily exist between them as shown in Fig. 7b,c [82].

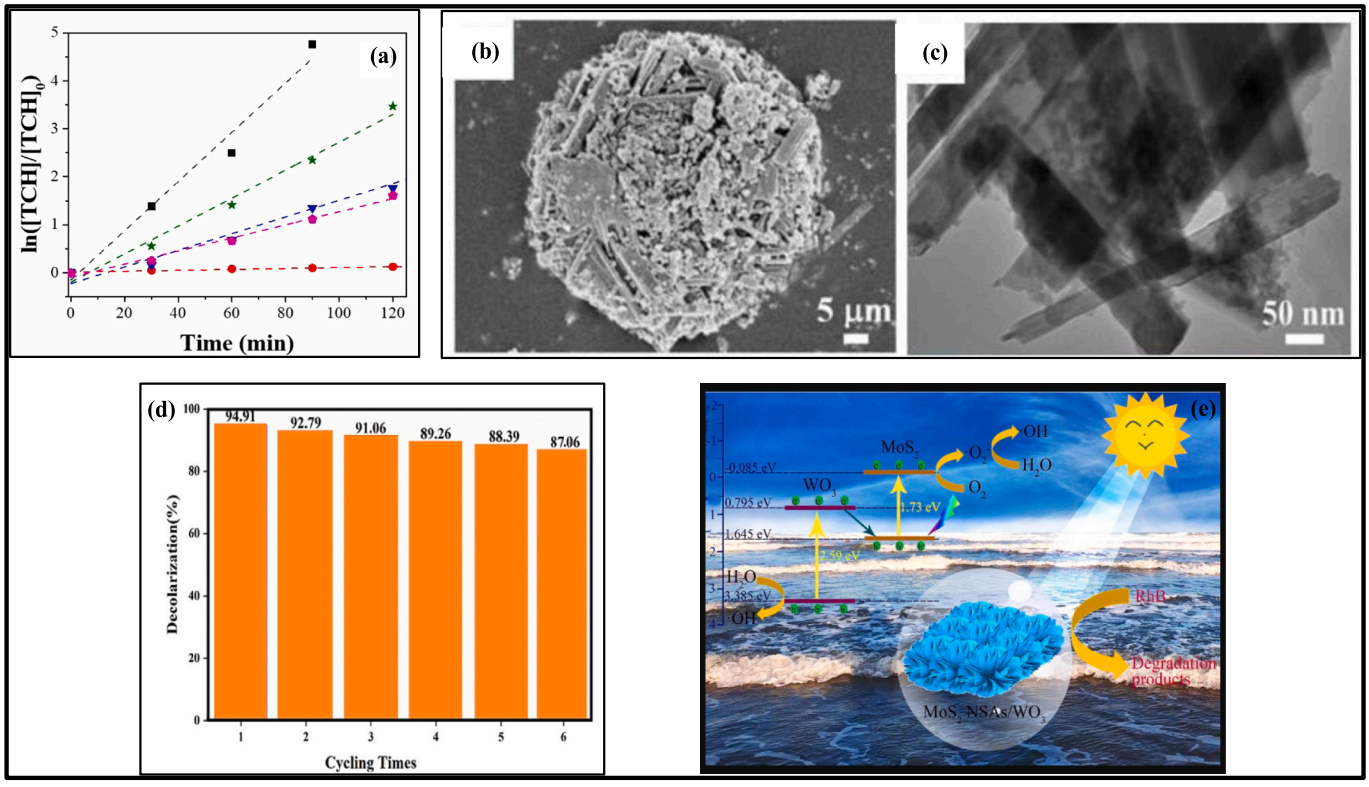


Fig. 7. a) Linear fit curves in the TCH degradation [144] b) SEM image of WO_3/CdS [82] c) HRTEM image of WO_3/CdS [82] d) Reusability of photocatalyst WO_3/CuS for six cycles [88] e) Schematic illustration of Photocatalytic Mechanism [153].

Phenazopyridine (PhP) is a tablet used as an antibiotic to relieve pain in the urinary tract but its toxicity and carcinogenic properties proved to be a source of water pollution which is dangerous for aquatic as well as human beings' lives. Therefore, the WO_3/CdS composite has also been used for the removal of this drug because there was less recombination rate of electron-hole pair, and the process of transferring electrons and holes was faster in this heterojunction. So, the composite was subsequently employed in the photodegradation of phenazopyridine drug in an aqueous solution, and it showed up to 90 % degradation efficiency of PhP under 45 min [150].

6.2. WO_3/other transition metal sulfides heterojunctions

CuS is a transition metal sulfide and is used to form a nano-composite with WO_3 because of its strong optical, electrical, and availability properties. WO_3 is used in photocatalytic, electrodes, and polarizing filter technology [151]. Although WO_3 possesses a visible light band gap, its high coupling rate of electron and hole pairs makes it an unsuitable photocatalyst for viable use. Adding CuS may change the material's band gap and provide trapping energy to lessen the rate of recombination, which could aid in the exclusion of different toxins from wastewater. A simple, straightforward, and efficient hydrothermal methodology was used to create WO_3/CuS nanoparticles. Some organic and non-biodegradable dyes are hazardous in the food, textile, and cosmetic sectors [152]. Therefore to remove these dyes heterojunction of WO_3/CuS has been formed which exhibits more efficient photocatalytic action than pure WO_3. The photocatalytic effectiveness of WO_3/CuS heterojunction was observed by its elimination efficiency against RhB which is 94.5 % under irradiation. The reason for higher degradation efficiency is the electron-hole pairs separation and the ability of more active sites for photocatalysis. Additionally, after using this photocatalyst for up to six cycles, there was a slight variation in the degrading efficiency shown in Fig. 7d [88]. Among transition metal sulfides MoS_2 is a dichalcogenide and it accepts electrons in different heterojunctions. WO_3/MoS_2 NCs have also been synthesized via hydrothermal method. WO_3/MoS_2 has remarkable significance because it has been widely used in photocatalysis and it forms *Z*-scheme heterojunction which includes efficient production, separation, and transportation of electron-hole charge carriers between two different semiconductors. When a heterojunction was used as a photocatalyst, there was 90 % removal of methylene blue dye during 60 min of light irradiation [89].

MoS_2 has a lower band gap than WO_3, and they can form Z-scheme heterojunctions, which is very effective for the elimination of various contaminants from polluted water. The values of the E_{VB} of WO_3 and MoS_2 were 3.54 and 1.73 eV, respectively, and the values of the E_{CB} were 0.64 and − 0.17 eV, respectively. In a Z-scheme heterojunction, an electric field has developed between two semiconductors, which efficiently transfer electrons and holes, and then these e/h pairs produce free radical species. These species degrade OPs and convert them into byproducts such as CO_2 and H_2O, as shown in Fig. 7e. MoS_2 nanosheet arrays with tungsten oxide can effectively degrade RhB up to 88.0 %. So, WO_3/MoS_2 heterojunction can be used on a large scale for disinfection of wastewater [153]. Thiamethoxam is an insecticide that is used in the field of agriculture to kill insects that feed on the roots and leaves of the plants but it is hazardous for living organisms. So, it is imperative to take action against it by using environment-friendly methods. The use of photocatalyst can be an effective way to eliminate such types of pesticides so after thorough studies researchers found out that WO_3/MoS_2 hybrid semiconductors can be used for degradation of TM pesticides due to the formation of junction between these two semiconductors and their band gap configuration. This hybrid material shows 90.20 %, and 92.60 % degradation efficiencies against TM and MB which proves that this heterojunction can be used in the future for photocatalysis [154].

7. Titanium oxide/metal sulfide heterojunctions

7.1. TiO_2/group 12 metal sulfide heterojunctions

Metal oxide such as Titanium dioxide (TiO_2) NCs have been recognized to be attractive photocatalyst options because of their appealing physicochemical qualities [155], for example, appropriate band location, nontoxicity, low-priced cost, and chemical and photonic stability of semiconductor [156]. The limitation of this semiconductor was a higher band gap (3.2 eV) therefore pristine TiO_2 is not commonly used for photocatalysis. Many methods have been suggested to improve its photocatalysis efficiency, like doping different metals and nonmetals and synthesizing its heterojunctions with other materials. Among metal sulfides, cadmium sulfide of Group 12 made a suitable heterojunction with TiO_2 because CdS has a low band gap (2.4 eV), making it suitable for photocatalysis [157]. The synthesized TiO_2/CdS heterostructure has a considerable photocatalytic performance for RhB deterioration (96.8 %) under light irradiation, and this higher degradation efficiency is due to the nanoporous morphology of TiO_2/CdS heterojunction, which not only provides an active region for the degradation process but also facilitates the transportation of photogenerated electron-hole pairs [158]. Aqueous chemical growth process has also been used to synthesize TiO_2/CdS heterojunction in which growth of CdS has been carried out on TiO_2 nanofibers (synthesized by electrospinning). The morphology of synthesized photocatalysts plays a prominent role in the removal of different hazardous contaminants. The synergistic effect of both semiconductors made it feasible to eliminate different dyes in examining through visible light irradiation. The model dyes MB, CR, and ER show 86 %, 96 %, and 91 % photodegradation efficiencies, respectively which is shown in Fig. 8a. With this degradation performance, TiO_2/CdS could be used more in practical work for the purification of wastewater [159]. ZnS has been used to make a junction with TiO_2 and due to this heterojunction efficient transfer of electron and hole charges is carried out with less recombination of these charges. A chemical vapor deposition approach was used to create TiO_2/ZnS NCs. The materials developed were evaluated as photocatalysts in the methylene blue decolorization process and it showed complete decolorization of methylene blue [160]. The degradation of orange II dye solutions under UV and vis. Radiation was moreover used to estimate the photocatalytic efficiency of TiO_2/ZnS composites. The heterojunction of TiO_2/ZnS shows higher degradation efficacy than individual ZnS and TiO_2 [161]. In another study, it has been reported that TiO_2/ZnS can also be used for removing pollutants produced during mineral processing. For example, Xanthate can be degraded up to 98.6 % using TiO2/ZnS as a photocatalyst under visible light [162].

7.2. TiO_2/other transition metal sulfide heterojunctions

In many industrial fields, Chromium (VI) has been used as a raw material, so there is a huge amount of chromium present in industrial water. Hexavalent Chromium is very dangerous for the health of human beings and other living bodies, and it is very difficult and toxic to deal with Cr (VI) containing pollutants. However, trivalent chromium is not so poisonous, so Chromium (VI) can be reduced to Cr (III) via a simple and facile method. Till now, many methods have been identified to manufacture different semiconductors which can be used in the reduction of Chromium (VI) into Cr (III), such as Bi-based (BiOBr/Bi_2S_3 [163], BiOI [164]) and Sn-based (Sn_3O_4) [165]. TiO_2/CuS unique heterostructure nanomaterial has applications in water treatment, dye pollution degradation, and environmental cleanup. The heterojunction TiO_2/CuS has been prepared by the hydrothermal method, and its working mechanism has been shown in Fig. 8b. The valence band and conduction band potentials of TiO_2 are calculated to be 3.04 and − 0.27 eV, respectively. The VB and the CB bottom of CuS are calculated to 1.51 and − 0.30 eV, respectively.TiO_2/CuS heterostructure also demonstrated promising applicability in the reduction of Cr (VI) contaminant

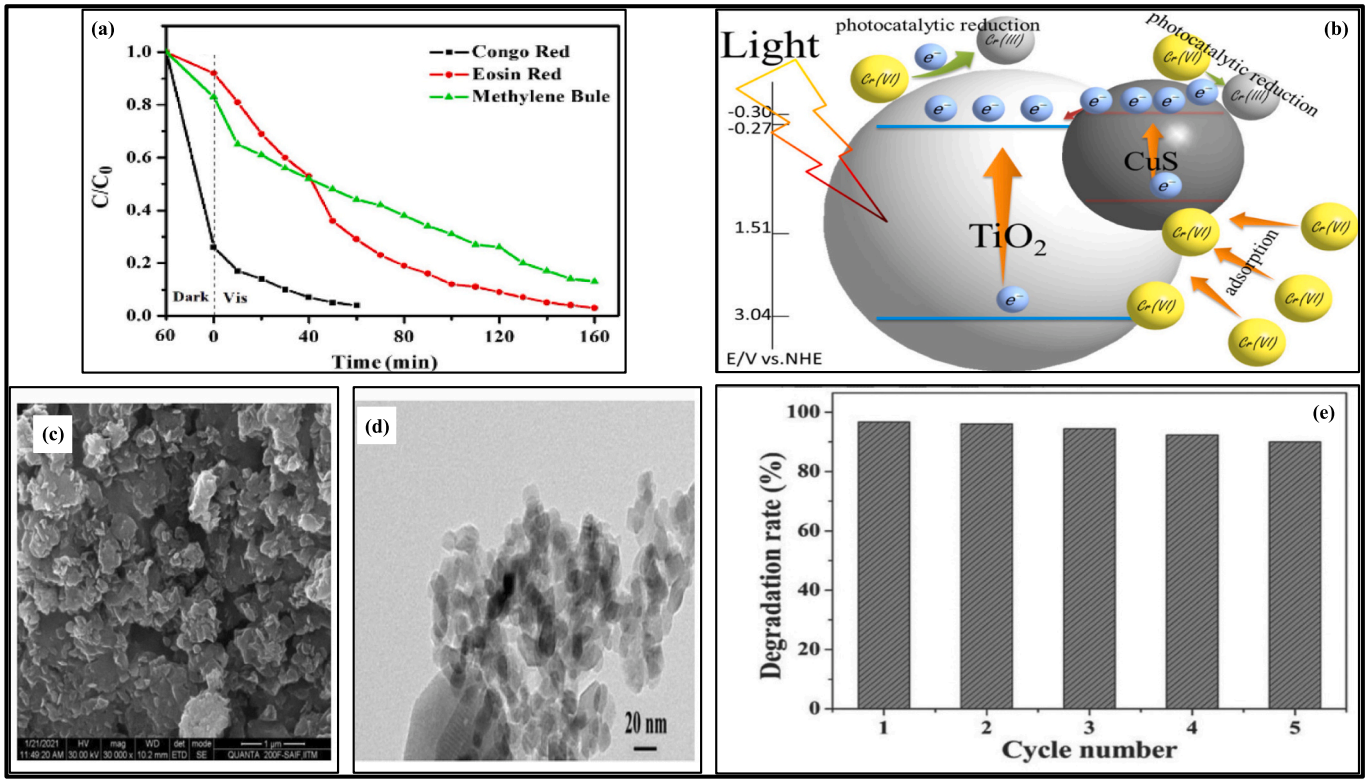


Fig. 8. a) Photodegradation rate of all dyes [159] b) the recommended Cr (VI) removal mechanism over TiO_2/CuS hierarchical structural design [96] c) SEM appearance of TiO_2/CuS [168] d) TEM appearance of TiO_2/CuS [168] e) Reusability cycles of degradation using TiO_2/MoS_2 [169].

(97 %) in aqueous media under illumination, and this is due to the availability of more electrons for the reduction of Cr (VI) to Cr (III) [96]. It is a thoughtful task to deposit metal sulfide on the exterior of TiO_2; therefore, direct deposition and bifunctional linker-assisted assembly are two alternative fabrication processes for the TiO_2/CuS heterojunction. Bifunctional linker DMSA has been used to bond CuS on the surface of titanium oxide semiconductor, and in the direct deposition method, no linker has been used, although only precursors to synthesize CuS and TiO_2 have been used. The heterojunction TiO_2@CuS synthesized by DMSA has 90 % of MB degradation efficiency, and TiO_2/CuS made by the direct deposition method has 76 % of MB degradation efficiency. Their photocatalytic performance under light exposure for the degradation rate of MB was compared [166].

Antibiotics are commonly used in daily life for human health so these are also excreted into the environment, which contaminates natural water used for drinking as well as for so many other purposes. So, it has become a serious problem to eliminate these antibiotics from the environment. One of the ways to this problem is to use semiconductor photocatalysts to degrade these antibiotics. TiO_2 has been widely used in degradation processes because it has a large surface space for photocatalysis but the drawback of this photocatalyst is a faster recombination rate and inefficient transfer of photogenerated charges. Therefore, CuS has been used with TiO_2 because CuS has a low bad gap (2.2 eV) and it enhances the degradation efficiency of photocatalyst. Enrofloxacin (ENR) is also an antibiotic and its presence in water causes pollution so for degradation ENR heterostructure TiO_2/CuS has been used. The TiO_2/CuS NBs have been used to remove ENR up to 85.5 % under visible light irradiation. Furthermore, this TiO_2/CuS heterostructure has a remarkable photocatalyst reusability and stability [167].

Crystal Violet dye has many applications in paper and textile industries. It has also been used in ballpoints, inks used in printers and fertilizers, etc. However, its harmful effects are reducing its usability in different industries because it causes cancer and eye diseases in living organisms. So, to eradicate CV dye from water TiO_2/CuS heterostructure has been used and it shows degradation efficiency of about 78.5 % under 60 min. This was owing to the lowering of the band gap of TiO_2 by incorporating a semiconductor CuS, which has a lower band gap, and electrons from CuS moved towards the conduction region of TiO_2, and holes from TiO_2 have shifted to CuS; these electron-hole pairs form active species like oxygen and hydroxyl radicals, which degrade dye and form non-toxic products. The morphology of this photocatalyst has also been shown in Fig. 8c,d [166,168].

Dichalcogenides have been considered effective photocatalysts due to their small bandgap like in the case of MoS_2. TiO_2/MoS_2 core-shell heterostructures have been created by a hydrothermal approach and have a larger surface area than pure TiO_2 due to their morphology in which nanosheets of MoS_2 have been raised on the outer surface of TiO_2, which may improve RhB dye adsorption. Under natural light illumination, the TiO_2/MoS_2 heterostructure attained 97.8 % degradation efficiency after 180 min. Moreover, this heterostructure shows cyclic stability, which proves that it can be used for many cycles with a small change in its degradation efficiency, as shown in Fig. 8e [169]. A solvothermal approach has been used to prepare a dual-function heterojunction catalyst, i.e., TiO_2/MoS_2. It has been used in the removal of ciprofloxacin, and an analysis of hydrogen production has also been carried out [170]. As previously discussed, Chromium (VI) is a common and dangerous contaminant in industrial water, and photocatalytic reduction is a suitable method for mitigating this contaminant. The TiO_2/SnS_2 hybrid nanostructure has the efficiency to convert Cr (VI) to its harmless form, i.e., Cr (VI). A suitable amount of TiO_2 is added to SnS_2 to form a heterojunction, and the synthesized composite exhibits stability up to 5 cycles with low loss of degradation efficiency (98 %) [171]. An additional interesting investigation has been conducted to determine the photocatalysts' performance in the presence of visible light and sunlight. TiO_2/FeS_2 photocatalyst was created using a wet chemical technique, and iron sulfide nanoparticles were evenly distributed across titanium oxide. Furthermore, this combination disintegrates methylene blue in visible light and sunlight by 97.2 % and

100 %, respectively [172].

In the end, it has been concluded that TiO_2 can be used to form heterojunctions with different metal sulfides, and they can be effectively used in environmental cleanup. TiO_2/CdS proves an effective catalyst for many reasons one of the reasons is its synthesis method. SILAR and chemical growth methods have been used to synthesize this photocatalyst which provides its nanoporous and fibrous shape. This shape provides boundaries for the efficient transfer of electron and hole pairs between two semiconductors and makes an efficient heterojunction. TiO_2/CuS has applications in removing and reducing Chromium ions because it provides surface area for the adsorption and reduction of chromium ions and it also shows the stability of photocatalyst. It is a very serious problem to deposit any meal sulfide on the surface of the catalyst therefore DMSO has been used as a linker to make a heterojunction between TiO_2 and CuS.

8. Other metal oxide/metal sulfide heterojunctions

There are so many other metal oxides/metal sulfides that have been prepared by different scientists and researchers. Some of which are discussed here. SnO_2/CdS heterojunction has been prepared by incorporating QDs of CdS into SnO_2 which increases its surface region and provides active spaces for photocatalysis [173]. CdS has a low bandgap and its conduction band potential appears more negative than the conduction band of SnO_2 so it transfers electrons to the conduction band of SnO_2 and holes are transferred to the valence region of SnO_2 and then these electrons and holes produce radical species which degrade pollutants The degradation efficiencies of SnO_2/CdS heterojunction against MB is 94 % under natural light and 90 % under UV irradiation [174]. In another study, SnO_2/CdS has been examined for the efficient reduction of Chromium (VI) and 82 % removal of TC antibiotic. So, this heterojunction can be used for a variety of removal of different OPs and it has diverse applications [175]. The hydrogel beads base on Bi_2O_2S/Bi_5O_7I/ZA have been efficiently used for the photocatalytic removal of elemental mercury up to 95 %. The results suggested that the appropriate ratio of Bi_2O_2S is crucial for higher activity, emphasizing the synergistic effect between the components [176]. SiO_2 is also an environment-friendly catalyst but its high band gap limits its photocatalytic activity, therefore a material that has a low band gap is required to incorporate it. ZnS has a low bandgap and it has been used to form a heterojunction with SiO_2 and then SiO_2/ZnS show remarkable efficiency against MB and eosin dyes under UV light source [177]. Hematite (α-Fe_2O_3) is an appealing material owing to its strength, cost-effectiveness, non-toxicity, abundance, and easiness of manufacture [178]. α-Fe_2O_3 is a promising visible-light photocatalyst with a low range of bandgap value of 2–2.2 eV. It utilizes the majority of sunlight and can serve as a photocatalyst [179]. However, it is significant to note that Fe_2O_3 has a limited electron-hole pair lifetime, which lowers the material's overall efficiency. MoS_2 can be utilized to create binary composites with Fe_2O_3 because of its layered structure, which allows it to offer surface area for photocatalysis. Because of its great light absorption, the heterojunction Fe_2O_3 /MoS_2 may degrade MB with an efficiency of 84 %. MoS_2 QDs have been utilized to create heterojunctions because they are more efficient than MoS_2 sheets or bulk MoS_2. Additionally, QDs offer more active atoms for photocatalysis and exhibit greater stability in aqueous conditions [180].

Scientists are also interested in magnetic iron oxide nanoparticles (IONP) due to their low valence band and ability to create type II heterojunctions. However, it is difficult to recover and separate these nanoparticles; thus, they can be combined with CdS to generate heterojunctions. In this manner, it is possible to synthesize IO/CdS, a recyclable and photostable photocatalyst that functions well in solar light. The photocatalytic efficiency of this catalyst was examined against Xylenol blue, and it demonstrated 97.6 % degrading efficiency. Furthermore, the antibacterial activity of IO/CdS NCs against the gram-positive bacterium *Staphylococcus aureus* was investigated for the first time in both dark and light conditions [181]. Aqueous Cr (VI) reduction through semiconductor photocatalytic reduction is an encouraging method due to its exceptional features, which include: (i) cost-effectiveness; (ii) direct utilization of free, hygienic, and safe natural energy; (iii) recyclability and (iv) no release of undesirable and toxic chemicals;. The resultant product is often Cr (III), which is much less hazardous than Cr (VI) and can certainly precipitate in neutral and alkaline solutions. SnS_2 is a reasonable and harmless photocatalyst exhibiting a bandgap of 2.0–2.25 eV that operates under visible light. SnO_2 is a stable broad bandgap photocatalyst (Eg = 3.56 eV) and it can form a heterojunction with SnS_2 due to their corresponding band potentials. So, SnO_2/SnS_2 can be utilized to reduce chromium (VI) to its non-hazardous form Cr (III), and it also demonstrates stability up to seven photocatalytic cycles [182]. CdO was preferred for its great natural stability, widespread accessibility, and inexpensive cost, and it has been used in a variety of important real-world applications. Zinc sulfide (ZnS) is also an essential semiconducting substance with numerous applications. As a result, a suitable combination of CdO/ZnS results in improved hybrid photocatalytic activity, the high specific capacitance of materials, and structural stability. Furthermore, due to the interface effect between two semiconductors i.e. CdO and ZnS, this photocatalyst exhibits a 92 % degradation effectiveness against the RhB dye. Furthermore, the stability of this hybrid composite has been studied, and only a slight variation in degrading efficiency has been found. After four cycles, 91 % efficiency has been achieved [183]. A comprehensive overview of different binary heterojunction photocatalysts of MOx/MS for degradation of various organic pollutants are presented in Table 1.

9. Demerits of MOx/MS

- A large number of metal sulfides (e.g., CdS, ZnS) easily undergo photocorrosion when exposed to light, diminishing their photocatalytic activity and their long-term stability [188].
- Some MOx/MS systems are not very stable at very acidic or basic conditions, and this restricts their applications to various types of wastewater [189].
- The use of some metal sulfides (e.g., CdS or PbS) can add toxic metal ions (e.g., Cd^{2+}, Pb^{2+}) into water [190]. Some health agencies have also warned that some nanoparticles may be carcinogenic (e.g., TiO_2) [191].
- Optimization of MOx/MS heterostructures composition and interfacial contact needs precise synthesis approaches [192], which may not be scalable and cost-efficient

10. Conclusion

In summary, heterojunctions of metal oxides and metal sulfides are a useful method for degrading organic contaminants. In comparison to a single semiconductor catalyst, the MOx/MS binary heterojunction has numerous advantages, including the separation and transportation of photoinduced charge carriers. The present review makes it clear that heterojunction creation essentially transforms the composites' overall shape, enhances their specific surface area (SSA), and changes their electrical structure to make them ideal for high-performance photocatalysis. A detailed discussion has been held over the combination of metal oxides and metal sulfides to form numerous kinds of binary heterojunction photocatalysts, their morphologies, and degradation efficiencies to degrade diverse organic contaminants. The research findings suggested that MOx/MS heterojunctions have greater mechanical and thermal stability [193] when contrasted with pristine [194] and it also underlined the interesting potential of metal oxide/metal sulfides heterojunctions as change agents in environmental sustainability and pollution management. These heterojunctions give particular responses to various classes of contaminants and provide a glimpse of the future in which they will be essential in reducing environmental problems. While there have been encouraging developments in the study of metal oxides/

Table 1
Efficient functioning of binary heterojunction photocatalysts based on MOx/MS for degradation of various organic pollutants.

Heterojunctions		Morphology	Synthesis Method	Light Source	Target Material	Degradation Efficiency	References
Copper Oxide/ Metal Sulfide	CuO/ FeS_2	NCs	Hydrothermal Method	Visible Mercury Halide lamp	BG Dye	95 %	[84]
	CuO/ CuS	Core-Shell Nanowires	Sulfidation Process	Visible	RhB	61 %	[107]
		Nanowires	Thermal oxidation and two-step annealing	Visible	MB	89 %	[106]
	CuO/ ZnS	Heterojunctions	Co-precipitation	Visible	MB, MO, MR	98.3 %, 94.2 %, and 92.8 %,	[57]
	CuO/ MoS_2	Heterojunctions	Hydrothermal	Visible	Methyl Violet, RhB	99.8 %, 95.3 %	[85]
		Flower-like Heterojunctions	Hydrothermal and calcination approach	Visible	2-mercaptobenzothiazole (MBT)	96 %	[69]
	CuO/ CdS	NCs	Thermal Oxidation And SILAR	UV–Visible	MB	94 %	[108]
		NCs	Ultrasound-assisted wet-impregnation approach	Visible	RhB, Methylene Blue, Methyl blue, MO	93 %, 75 %, 83 %, 80 %	[58]
	CuO/ TiS_2	Nano-Disc	CVT Method	Visible	MB	83.18 %	[184]
Zinc Oxide/ Metal Sulfides	ZnO/ ZnS	Hollow Nanorods	Hydrothermal Method	Visible	MB	96 %	[49]
		Nanowires	Solvothermal, Hydrothermal Methods	UV	MB, RhB	98.5 %, 87.5 %	[120]
		Nanocomposites	Biosynthesis Method	Dark	MB	87.61 %	[123]
		Spherical	Hydrothermal Method	Visible	MB	95.3 %	[124]
		Polycrystalline	Solid state Chemical Method	UV	MO, RhB, and TC	96 %,94 %, 93 %,	[122]
	ZnO/ CuS	Nanocomposite	Precipitation Method	Visible	Congo red dye and Phenol OPs	82 %	[129]
		1D heterostructure	Wet Chemical Method	Visible	MB	87 %	[93]
	ZnO/ TiS	Nanocomposite	Co-Precipitation	UV	TB	95 %	[94]
	ZnO/ FeS_2	NCs	Chemical Precipitation Method	UV	MG	98.0 %	[136]
	ZnO/ MoS_2	Flower-like Nanosheets	Hydrothermal Method	Visible	MB	67 %	[86]
	ZnO/ Ag_2S	Agglomerated Irregular NCs	Combustion Method	Visible	Tetracycline	87.50 %	[185]
			Sol-Gel Method	Visible	Acid Black 1	84.5 %	[98]
	ZnO/ CdS	Polycrystalline Granular Nanostructures	Co-Precipitation	Visible	MB	99 %	[92]
		Flower Like Nanostructures	Wet Chemical Method	UV	RhB	80 %	[186]
		Quasi Spherical	Hydrothermal method	Visible	MB	90.5 %	[124]
		Nanorods	Aqueous Chemical Growth	Visible	3,4-dihydroxy benzoic acid	–	[133]
	ZnO/ SnS_2	Nanospheres like porous Composites	Microwave-assisted Method	Visible	Ciprofloxacin Antibiotic, Methylene Blue, Chromium ion	90.2 %, 98.2 %, 80.2 %	[137,138]
	ZnO/ PbS	Flower-Like Flake	Hydrothermal Method	Visible	MB	89.4 %	[124]
	ZnO/ NiS	Irregular	Combustion	Visible	Tetracycline	77.27 %	[185]
		Spherical	Hydrothermal	UV-light (8 W)	p-nitrophenolate, RhB	96 %,93 %	[87]
Tungsten Oxide/ Metal Sulfides	WO_3/ ZnS	Heterojunctions	Hydrothermal	UV–Visible	TC Antibiotic	–	[144]
		NCs	Precipitation Method	Visible(Xenon Lamp)	Uranium VI	93.4 %	[95]
	WO_3/ CuS	Nanorods	Hydrothermal	Visible	RhB	94.9 %	[88]
	WO_3/ CdS	NCs	Hydrothermal And Precipitation Method	Visible (Xenon Lamp)	Imidacloprid (IMD) pesticide	80 %	[82]
		NCs	Precipitation Method	Visible (Tungsten Lamp)	Phenazopyridine (PhP) drug	90 %	[150]
	WO_3/ MoS_2	NCs	Hydrothermal	Visible (CDM-R lamp)	MB	90 %	[89]
		Nanosheets arrays	Hydrothermal method	Visible	RhB	88.0 %	[153]
		NCs	Hydrothermal method	Visible	TM and RhB	90.02 %, 92.60 %	[154]
Titanium Oxide/ Metal Sulfides	TiO_2/ CuS	Heterojunctions	Precipitation	Visible (Metal Halide Lamp)	Chromium Cr(VI)	97 %	[96]
		NCs	Direct deposition and bifunctional linker-assisted	Visible(W Xenon Lamp)	MB	76 %,90 %	[166]
		Nanobelts	SILAR Method	Solar Light	Antibiotic Enrofloxacin (ENR)	85.5 %	[167]
		NCs	Hydrothermal	Visible W lamp	Crystal Violet (CV) Dye	78.35 %	[168]

(*continued on next page*)

Table 1 (*continued*)

Heterojunctions		Morphology	Synthesis Method	Light Source	Target Material	Degradation Efficiency	References
	TiO_2/ MoS_2	NCs	Solvothermal	UV–Visible	Ciprofloxacin	93 %	[170]
		Nanobelts	Hydrothermal	Visible (W Xenon Lamp)	RhB	97.8 %	[169]
	TiO_2/ CdS	Nanohybrids	Electrospinning and SILAR	Visible	RhB	96.8 %	[158]
		Heteronanofibers	Electrospinning and Hydrothermal	Visible	MB, CR, ER	86 %,96 %,91 %	[159]
	TiO_2/ ZnS	NCs	Chemical Vapor Deposition	Visible	MB	100 %	[160]
		Nano spherical	Solvothermal method	Visible	Xanthate	98.6 %	[162]
		NCs	Homogeneous hydrolysis	UV And Visible	Orange II	–	[161]
	TiO_2/ FeS_2	NCs	Sonochemical	Visible	RhB	97 %	[187]
		Nanocrystals	Wet Chemical	Sunlight Visible	MB	100 %, 97.2 %	[172]
	TiO_2/ SnS_2	Nanoflakes	Solvothermal	Visible	Cr (VI)	–	[171]
Other Metal Oxides/Metal Sulfides	SnO_2/ CdS	Crystalline	Sol-Gel	UV Visible	MB	90 %,94 %	[174]
		Monodisperse	Hydrothermal	Visible	Cr (VI) TC	95 %,82 %	[175]
	SiO_2/ ZnS	Heterostructure	Sol-Gel	UV	ES MB	97 %	[177]
	SnO_2/ SnS_2	Nanorods decorated on Nanoflakes	Hydrothermal	Visible	Cr(VI)	–	[182]
	CdO/ ZnS	Crystalline	Co-precipitation	UV	RhB	92 %	[183]
	IO/CdS	Core/Shell Nanocrystals	Sequential one-pot method	Visible	Xylenol blue (XB)	97.6 %	[181]
	CeO_2/ ZnS	Spherical	Precipitation Method	Visible	CV	93.8 %	[35]
	Fe_2O_3/ MoS_2	QDs form agglomeration	Ultrasonic Method	Visible	MB	84 %	[180]

metal sulfides heterojunction photocatalysts, there are still numerous serious issues that need to be resolved. Finally, more research will be required to create and manufacture highly efficient MOx/MS heterojunction photocatalysts for practical applications.

11. Future perspectives

1. Synthesis of multifunctional heterojunctions will be able to address multiple environmental challenges simultaneously.
2. Improving the efficiency of binary heterojunction photocatalysts by selecting suitable materials that can enhance their rate of degradation.
3. Develop synthesis methods and manufacturing processes that will be suitable for mass production considering economic and industrial feasibility.
4. Optimization of the relative concentrations of different semiconductors, as well as determination of the accurate location of active sites will most probably increase degradation efficiency.
5. When a two-component heterojunction photocatalyst is upgraded to a multi-component heterojunction photocatalyst, the effectiveness of photocatalysis increases under the irradiation of natural light.
6. Integration of metal oxide/metal sulfides heterojunctions with other advanced nanomaterials, such as carbon-based nanomaterials (graphene, carbon nanotubes), will create hybrid NCs with enhanced properties for environmental and energy applications.
7. Developing low-cost, accessible, and green synthesis techniques will reduce overall management costs.

CRediT authorship contribution statement

Atiqa Aslam: Writing – original draft, Investigation, Data curation. **Nimra Nadeem:** Writing – original draft, Visualization, Validation. **Balaussa Balgabayeva:** Software, Formal analysis. **Sami Ullah Khan:** Visualization, Methodology. **Qamar Abbas:** Validation, Formal analysis, Conceptualization. **Saima Noreen:** Resources, Investigation. **Muhammad Zahid:** Writing – review & editing, Supervision, Conceptualization. **Zhazira Supiyeva:** Writing – review & editing, Project administration, Funding acquisition.

Declaration of competing interest

The authors declare that they have no known competing financial interests or personal relationships that could have appeared to influence the work reported in this paper.

Acknowledgements

This research has been funded by the Committee of Science of the Ministry of Science and Higher Education of the Republic of Kazakhstan (Grant No. BR27198045).

Data availability

No data was used for the research described in the article.

References

[1] H. Chen, et al., A deep learning CNN architecture applied in smart near-infrared analysis of water pollution for agricultural irrigation resources, Agric. Water Manag. 240 (2020) 106303.
[2] J. Li, S. Li, Energy investment, economic growth and carbon emissions in China—empirical analysis based on spatial Durbin model, Energy Policy 140 (2020) 111425.
[3] Z. Wu, Q. Ye, Water pollution loads and shifting within China's inter-province trade, J. Clean. Prod. 259 (2020) 120879.
[4] S. Ali, et al., *Water Pollution: Diseases and Health Impacts*, in *Freshwater Pollution and Aquatic Ecosystems*, Apple Academic Press, 2021, pp. 1–23.

[5] G.F. Vasse, B.N. Melgert, Microplastic and plastic pollution: impact on respiratory disease and health, Eur. Respir. Rev. 33 (172) (2024).
[6] T. Münzel, et al., Soil and water pollution and cardiovascular disease, Nat. Rev. Cardiol. 22 (2) (2025) 71–89.
[7] Z. Pan, T. Gong, P. Liang, Heavy metal exposure and cardiovascular disease, Circ. Res. 134 (9) (2024) 1160–1178.
[8] H.-J. Lin, et al., Arsenic levels in drinking water and mortality of liver cancer in Taiwan, J. Hazard. Mater. 262 (2013) 1132–1138.
[9] T. Farkhondeh, et al., Drinking water heavy metal toxicity and chronic kidney diseases: a systematic review, Rev. Environ. Health 36 (3) (2021) 359–366.
[10] S.E. Bresson, J. Ruzzin, Persistent organic pollutants disrupt the oxidant/antioxidant balance of INS-1E pancreatic β-cells causing their physiological dysfunctions, Environ. Int. 190 (2024) 108821.
[11] A. Saravanan, et al., Effective water/wastewater treatment methodologies for toxic pollutants removal: processes and applications towards sustainable development, Chemosphere 280 (2021) 130595.
[12] S.A.R. Khan, et al., Environmental technology and wastewater treatment: strategies to achieve environmental sustainability, Chemosphere 286 (2022) 131532.
[13] B. Zhang, et al., Piezoelectric effect coupled advanced oxidation processes for environmental catalysis application, Coord. Chem. Rev. 523 (2025) 216234.
[14] A. Kumar, et al., Controlled synthesis of nanosized cd-CeO2 for efficient pH responsive photocatalytic degradation of CV dye for sustainable wastewater treatment, Mater. Sci. Eng.: B 311 (2025) 117840.
[15] M. Rani, U. Shanker, V. Jassal, Recent strategies for removal and degradation of persistent & toxic organochlorine pesticides using nanoparticles: a review, J. Environ. Manage. 190 (2017) 208–222.
[16] A. Sarkar, B. Das, S. Basumatary, Trending applications of layered triple hydroxide composites in adsorption and photocatalysis for highly effective wastewater treatment, Inorg. Chem. Commun. 174 (2025) 114052.
[17] R. Gusain, et al., Adsorptive removal and photocatalytic degradation of organic pollutants using metal oxides and their composites: a comprehensive review, Adv. Colloid Interface Sci. 272 (2019) 102009.
[18] S. Yadav, N. Rani, K. Saini, A review on transition metal oxides based nanocomposites, their synthesis techniques, different morphologies and potential applications, in: IOP Conference Series: Materials Science and Engineering, IOP Publishing, 2022.
[19] J. Xiao, et al., Flash joule heating synthesis of nitrogen-rich defective G-C_3N_4 for highly efficient photocatalytic hydrogen evolution, Small (2025) 2503335.
[20] V.T. Rathod, J.S. Kumar, A. Jain, Polymer and ceramic nanocomposites for aerospace applications, Appl. Nanosci. 7 (2017) 519–548.
[21] S. Jabeen, et al., A comprehensive review on metal oxide-based nanomaterials: synthesis, characterization, environmental, and therapeutic applications, ChemistrySelect 10 (11) (2025) e202500080.
[22] M. Xie, et al., Long-lived, visible-light-excited charge carriers of TiO2/BiVO4 nanocomposites and their unexpected Photoactivity for water splitting, Adv. Energy Mater. 4 (5) (2014) 1300995.
[23] S. Gautam, et al., Metal oxides and metal organic frameworks for the photocatalytic degradation: a review, J. Environ. Chem. Eng. 8 (3) (2020) 103726.
[24] M. Parashar, V.K. Shukla, R. Singh, Metal oxides nanoparticles via sol–gel method: a review on synthesis, characterization and applications, J. Mater. Sci. Mater. Electron. 31 (2020) 3729–3749.
[25] S.R. Mishra, M. Ahmaruzzaman, CuO and CuO-based nanocomposites: synthesis and applications in environment and energy, Sustain. Mater. Technol. 33 (2022) e00463.
[26] M. Belikov, S. Safaryan, P. Korneikova, Synthesis of titanium oxide/manganese oxide composites and their physicochemical and photocatalytic properties, Inorg. Mater. 59 (2) (2023) 145–156.
[27] M. Sołtys-Mróz, et al., Band gap engineering of nanotubular Fe2O3-TiO2 photoanodes by wet impregnation, Appl. Surf. Sci. 517 (2020) 146195.
[28] H. Shukla, R. Gautam, N. Kumari, A comprehensive review: photodegradation of dyes with rare earth doped metal oxide nanoparticles for wastewater treatment, J. Phys. Chem. Solid 200 (2025) 112593.
[29] S. Chandrasekaran, et al., Recent advances in metal sulfides: from controlled fabrication to electrocatalytic, photocatalytic and photoelectrochemical water splitting and beyond, Chem. Soc. Rev. 48 (15) (2019) 4178–4280.
[30] H. Guo, et al., Enhancing H2 evolution activity of MWCNTs-biphasic CdS photocatalyst through microstructure regulation, J. Environ. Chem. Eng. 13 (3) (2025) 116417.
[31] S. Khan, et al., Challenges and innovative strategies related to synthesis and electrocatalytic/energy storage applications of metal sulfides and its derivatives, J. Electroanal. Chem. 923 (2022) 116760.
[32] P. Dharmalingam, et al., Synthesis of metal oxides/sulfides-based nanocomposites and their environmental applications: a review, Mater Today Sustain. 20 (2022) 100232.
[33] X. Duan, et al., Study on the sterilization performance of Photocatalysts used in indoor air purification, Indoor Air 2025 (1) (2025) 1071778.
[34] S. Yadav, et al., Chapter 9 - Interface dynamics in metal sulfides and metal oxides for photodegradation of organic contaminants, in: P.R. Makgwane, N. Kumar (Eds.), Metal Sulfide Nanomaterials for Environmental Applications, Elsevier, 2025, pp. 217–234.
[35] S. Kaliyamoorthy, G. Murugadoss, S. Salla, Rapid photocatalytic degradation of selective organic dyes using metal oxide-metal sulphide and its inverted nanocomposites, Inorg. Chem. Commun. 172 (2025) 113668.
[36] X. He, T. Kai, P. Ding, Heterojunction photocatalysts for degradation of the tetracycline antibiotic: a review, Environ. Chem. Lett. 19 (6) (2021) 4563–4601.
[37] Z. You, et al., Organic-inorganic PVDF/Zn0.5Cd0.5S/Ti-NT photocatalytic membrane with synergistic effect of heterojunction and its derived multi-element excitation NO purification, Sep. Purif. Technol. 361 (2025) 131293.
[38] M. Zahid, et al., Multifunctional Hybrid Nanomaterials for Sustainable Agri-Food and Ecosystems, Elsevier Amsterdam, The Netherlands, 2020.
[39] T. Shen, M. Gao, Gemini surfactant modified organo-clays for removal of organic pollutants from water: a review, Chem. Eng. J. 375 (2019) 121910.
[40] X. Li, et al., A novel strategy to construct a visible-light-driven Z-scheme (ZnAl-LDH with active phase/g-C3N4) heterojunction catalyst via polydopamine bridge (a similar“ bridge” structure), J. Hazard. Mater. 386 (2020) 121650.
[41] Y. Zong, et al., Functionalized separator strategies toward advanced aqueous zinc-ion batteries, Adv. Energy Mater. 13 (20) (2023) 2300403.
[42] X. Zhang, et al., Powerful combination of 2D g-C3N4 and 2D nanomaterials for photocatalysis: recent advances, Chem. Eng. J. 390 (2020) 124475.
[43] K. Song, et al., Metal-organic framework materials in NH3-SCR: progress and prospects, Coord. Chem. Rev. 535 (2025) 216615.
[44] A. Balakrishnan, G.J. Gaware, M. Chinthala, Heterojunction photocatalysts for the removal of nitrophenol: a systematic review, Chemosphere 310 (2023) 136853.
[45] S.A. Younis, E. Amdeha, R.A. El-Salamony, Enhanced removal of p-nitrophenol by β-Ga2O3-TiO2 photocatalyst immobilized onto rice straw-based SiO2 via factorial optimization of the synergy between adsorption and photocatalysis, J. Environ. Chem. Eng. 9 (1) (2021) 104619.
[46] H. Zhou, et al., Towards highly efficient photocatalysts using semiconductor nanoarchitectures, Energ. Environ. Sci. 5 (5) (2012) 6732–6743.
[47] J. Low, et al., Heterojunction photocatalysts, Adv. Mater. 29 (20) (2017) 1601694.
[48] P.V. Pham, et al., 2D heterostructures for ubiquitous electronics and optoelectronics: principles, opportunities, and challenges, Chem. Rev. 122 (6) (2022) 6514–6613.
[49] P. Kumari, S. Pande, P. Fageria, Facile synthesis of ZnO/ZnS hollow nanorods via Kirkendall effect with enhanced photocatalytic degradation of methylene blue, Environ. Sci. Pollut. Res. 30 (22) (2023) 61927–61944.
[50] X. Jiang, et al., A novel strategy to construct the superior performance of 3D multi-shell CeO2/ZnO@ZnS as a reusable sunlight-driven ternary photocatalyst for highly efficient water remediation, J. Environ. Chem. Eng. 9 (4) (2021) 105608.
[51] D. Ma, et al., An ultrathin Al 2 O 3 bridging layer between CdS and ZnO boosts photocatalytic hydrogen production, J Mater Chem A 8 (21) (2020) 11031–11042.
[52] Y. Zhong, et al., Interface engineering of heterojunction photocatalysts based on 1D nanomaterials, Cat. Sci. Technol. 11 (1) (2021) 27–42.
[53] H. Wang, et al., A review on heterogeneous photocatalysis for environmental remediation: from semiconductors to modification strategies, Chin. J. Catal. 43 (2) (2022) 178–214.
[54] V. Hasija, et al., Step-scheme heterojunction photocatalysts for solar energy, water splitting, CO 2 conversion, and bacterial inactivation: a review, Environ. Chem. Lett. 19 (2021) 2941–2966.
[55] M. Arunkumar, et al., A novel visible light-driven p-type BiFeO3/n-type SnS2 heterojunction photocatalyst for efficient charge separation and enhanced photocatalytic activity, J. Clust. Sci. 32 (5) (2021) 1431–1439.
[56] M. Tarek, et al., Photoelectrochemical activity of CuO-CdS heterostructured catalyst for CO2 reduction, in: IOP Conference Series: Materials Science and Engineering, IOP Publishing, 2020.
[57] M.P. Kumar, et al., Fabrication of dual-functional heterostructured p-CuO/n-ZnS nanocomposite for enhanced visible-light active photocatalytic response and fluorometric sensor for selective sensing of thiol-containing amino acids, Chem. Eng. Res. Des. 198 (2023) 92–104.
[58] S.S. Hossain, et al., Facile synthesis of CuO/CdS heterostructure photocatalyst for the effective degradation of dye under visible light, Environ. Res. 188 (2020) 109803.
[59] P. Kumari, et al., Engineering Schottky-like and heterojunction materials for enhanced photocatalysis performance–a review, Mater. Adv. 3 (5) (2022) 2309–2323.
[60] B. Luo, et al., Fabrication of a ag/Bi3TaO7 plasmonic photocatalyst with enhanced photocatalytic activity for degradation of tetracycline, ACS Appl. Mater. Interfaces 7 (31) (2015) 17061–17069.
[61] K. Cao, et al., Facile preparation of a 3D rGO/g-C3N4 nanocomposite loaded with Ag NPs for photocatalytic degradation, RSC Adv. 15 (22) (2025) 17089–17101.
[62] Q. Fang, et al., Recent advances in doping engineering of heterogeneous catalyst for carbon dioxide hydrogenation, Mater. Today Chem. 46 (2025) 102770.
[63] H. Wang, et al., Ti3C2 Mxene modified SnNb2O6 nanosheets Schottky photocatalysts with directed internal electric field for tetracycline hydrochloride removal and hydrogen evolution, Sep. Purif. Technol. 265 (2021) 118516.
[64] S. Jana, et al., Fabrication of a new heterostructure au/Pt/SnO2: an excellent catalyst for fast reduction of para-nitrophenol and visible light assisted photodegradation of dyes, Mater. Res. Bull. 141 (2021) 111351.
[65] A. Kumar, et al., Recent developments and challenges in practical application of visible–light–driven TiO2–based heterojunctions for PPCP degradation: a critical review, Water Res. 170 (2020) 115356.
[66] Y. Yang, et al., Flexible carbon-fiber/semimetal bi nanosheet arrays as separable and recyclable plasmonic photocatalysts and photoelectrocatalysts, ACS Appl. Mater. Interfaces 12 (22) (2020) 24845–24854.

[67] A. Kudo, H. Kato, I. Tsuji, Strategies for the development of visible-light-driven photocatalysts for water splitting, Chem. Lett. 33 (12) (2004) 1534–1539.
[68] Y. Ma, et al., Construction of Z-scheme system for enhanced photocatalytic H2 evolution based on CdS quantum dots/CeO2 nanorods heterojunction, ACS Sustain. Chem. Eng. 6 (2) (2018) 2552–2562.
[69] Y. Wang, et al., Fabrication of a Z-scheme MoS 2/CuO heterojunction for enhanced 2-mercaptobenzothiazole degradation activity and mechanism insight, New J. Chem. 44 (42) (2020) 18264–18273.
[70] K. Shi, et al., Oxygen vacancy-rich 2D/2D S-scheme photocatalyst CN/BiOBr-OV for efficient azo dye degradation, Sep. Purif. Technol. 360 (2025) 131092.
[71] Q. Han, et al., Built-in field-driven S-scheme boron-doped nanodiamond/TiO2 (101)/MXene photocatalyst for efficient antibiotic elimination: mechanisms and DFT validation, Chem. Eng. J. 519 (2025) 165290.
[72] Z. Wang, et al., Enhanced photocatalytic degradation of tetracycline under visible light via a novel S-scheme Zn3V2O8/ZnIn2S4 heterostructure construction, J. Alloys Compd. 1032 (2025) 181088.
[73] H. Ge, et al., S-scheme heterojunction TiO2/CdS nanocomposite nanofiber as H2-production photocatalyst, ChemCatChem 11 (24) (2019) 6301–6309.
[74] J. Song, et al., CuCo2O4/ZnS S-scheme heterostructure for ultrasound−/photo-assisted degradation of pollutants and their biological toxicity assessment, J Water Process Eng 75 (2025) 107929.
[75] S. Wang, K. Qi, Localized surface plasmon resonance effect in S-scheme photocatalyst, J. Mater. Sci. Technol. 226 (2025) 317–319.
[76] Y. Wu, et al., Efficient photocatalytic production of H2O2 over ZnO/D-A conjugated polymer S-scheme heterojunction and charge transfer dynamics investigation, Acta Phys. -Chim. Sin. 40 (11) (2024) 2406027.
[77] G. Mahalakshmi, M. Rajeswari, P. Ponnarasi, Synthesis of few-layer g-C3N4 nanosheets-coated MoS2/TiO2 heterojunction photocatalysts for photo-degradation of methyl orange (MO) and 4-nitrophenol (4-NP) pollutants, Inorg. Chem. Commun. 120 (2020) 108146.
[78] J. Zhang, et al., CuInS2 quantum-dot-modified g-C3N4 S-scheme heterojunction photocatalyst for hydrogen production and tetracycline degradation, J. Mater. Sci. Technol. 172 (2024) 145–155.
[79] X. Wang, et al., Synthesis of ZnWO4/NiWO4 photocatalysts and their application in tetracycline hydrochloride degradation and antibacterial activities, J. Taiwan Inst. Chem. Eng. 157 (2024) 105408.
[80] N.C. Joshi, P. Gururani, S.P. Gairola, Metal oxide nanoparticles and their nanocomposite-based materials as photocatalysts in the degradation of dyes, Biointerface Res. Appl. Chem 12 (2022) 6557–6579.
[81] K. Subramani, et al., Hydrothermally and green synthesized TiO2 nanoparticles with high photocatalytic textile industry dye degradation, antibacterial and antioxidant activities, J. Alloys Compd. 1017 (2025) 179068.
[82] J. Li, et al., Prominent dual Z-scheme mechanism on phase junction WO3/CdS for enhanced visible-light-responsive photocatalytic performance on imidacloprid degradation, Sep. Purif. Technol. 281 (2022) 119863.
[83] K.G. Motora, et al., Fabrication of super sensitive, stable and selective black TiO2 nanoforest-based room temperature H2 gas sensors by facile and simple hydrothermal method, Int. J. Hydrogen Energy 120 (2025) 44–53.
[84] A.G. Raju, et al., Fabrication of a heterostructure composite with CuO and FeS2 as efficient photocatalyst for decolourisation of brilliant green, J. Mater. Res. Technol. 17 (2022) 2648–2656.
[85] Yasin, U.A.A., et al., *Coupling of Mos2 with Cuo with Synergistic Effect for Enhanced Photodegradation of Organic Dyes Under Visible Light.* Available at SSRN 4402656.
[86] S. Karmakar, S. Ghosh, P. Kumbhakar, Enhanced sunlight-driven photocatalytic and antibacterial activities of flower-like ZnO@ MoS 2 nanocomposite, J. Nanopart. Res. 22 (2020) 1–20.
[87] S.K. Pandey, P.K. Mishra, D. Tiwary, Enhanced photocatalytic performance of NiS/ZnO nanocomposite for the remediation of PNP and RhB dye, J. Environ. Chem. Eng. 10 (3) (2022) 107459.
[88] M. Ashraf, et al., Experimental and theoretical verification of WO3 based nanocomposites for their application as efficient photo catalyst for treatment of industrial wastewater, J. Inorg. Organomet. Polym. Mater. (2023) 1–15.
[89] S. Shenoy, K. Sridharan, K. Tarafder, Remarkable Photocatalytic Behavior of WO3/MoS2 Heterostructure: Insights from a Combined Experimental and Theoretical Investigations, 2021.
[90] Y. Wang, et al., Visible light driven type II heterostructures and their enhanced photocatalysis properties: a review, Nanoscale 5 (18) (2013) 8326–8339.
[91] P.G. Jamkhande, et al., Metal nanoparticles synthesis: an overview on methods of preparation, advantages and disadvantages, and applications, J. Drug Deliv. Sci. Technol. 53 (2019) 101174.
[92] N. Saxena, et al., Equimolar ZnO-CdS nanocomposite for enhanced photocatalytic performance, Chem. Phys. Impact 5 (2022) 100119.
[93] M. Basu, N. Garg, A.K. Ganguli, A type-II semiconductor (ZnO/CuS heterostructure) for visible light photocatalysis, J Mater Chem A 2 (20) (2014) 7517–7525.
[94] Bharanidharan, M., S. Manivarman, and G. Prabakaran, *Exceedingly Resourceful in Hierarchically structured ZnO-TiS Nanocomposite material and its multi application.*
[95] N. Liu, et al., Z-scheme heterojunction ZnS/WO3 composite: photocatalytic reduction of uranium and band gap regulation mechanism, J. Colloid Interface Sci. 630 (2023) 727–737.
[96] Z. Wu, et al., Construct interesting CuS/TiO2 architectures for effective removal of Cr (VI) in simulated wastewater via the strong synergistic adsorption and photocatalytic process, Sci. Total Environ. 796 (2021) 148941.
[97] K. Rachana, et al., Third-order nonlinear optical properties of TiO2 nano colloidal synthesized via sol–gel and hydrothermal methods: a comparison, Mater. Sci. Eng. B 319 (2025) 118312.
[98] B. Subash, et al., An efficient nanostructured Ag2S–ZnO for degradation of acid black 1 dye under day light illumination, Sep. Purif. Technol. 96 (2012) 204–213.
[99] D. Wang, et al., Facile ball-milling synthesis of carbon nitride Z-scheme heterojunction for dramatically enhanced photocatalytic degradation of environmental pollutants, J. Photochem. Photobiol. A Chem. 469 (2025) 116546.
[100] M. Ye, et al., Effect of ball milling process on the photocatalytic performance of CdS/TiO2 composite, Nanotechnol. Rev. 9 (1) (2020) 558–567.
[101] M.J. Mezher, M.A. Kudhier, O.A. Dakhil, Using ZnO-CdS composite nanofibers in the photolytic activity under sunlight irradiation, arXiv preprint arXiv: 2301.05831, 2023.
[102] A.M. Ilyas, et al., Facile synthesis of titanium dioxide-cadmium sulfide nanocomposite using pulsed laser ablation in liquid and its performance in photovoltaic and photocatalytic applications, Int. J. Energy Res. 41 (10) (2017) 1422–1435.
[103] T. Wang, et al., Laser-induced photochemical synthesis of fibrous-shaped CuO@ CuS nanoporous structures for enhanced electrostatic adsorption of negatively charged contaminants from wastewater, Opt Mater Express 7 (11) (2017) 3863–3874.
[104] V. Hasija, et al., Recent advances in noble metal free doped graphitic carbon nitride based nanohybrids for photocatalysis of organic contaminants in water: a review, Appl. Mater. Today 15 (2019) 494–524.
[105] L. Fatolahi, Preparation of CuS/CuO on decoration graphene oxide nanocomposites for the photocatalytic degradation of gaseous phase based on UV light irradiation, and evaluation of toxicology on bacterial cells, J. Inorg. Organomet. Polym. Mater. 34 (5) (2024) 2030–2041.
[106] Y.-T. Kao, S.-M. Yang, K.-C. Lu, Synthesis and photocatalytic properties of CuO-CuS core-shell nanowires, Materials 12 (7) (2019) 1106.
[107] F. Cao, Z. Pan, X. Ji, Enhanced photocatalytic activity of a pine-branch-like ternary CuO/CuS/ZnO heterostructure under visible light irradiation, New J. Chem. 43 (28) (2019) 11342–11347.
[108] Y. Yang, et al., Thermal oxidation and SILAR method to prepare CuO/CdS composite nanostructure and its enhanced photocatalytic properties, J. Electron. Mater. 50 (2021) 4762–4769.
[109] C.L. Londoño-Calderón, et al., Synergistic effects in magnetically recoverable nanocomposites of CuO nanoleaves with Fe3O4 nanoparticles for organic dye degradation, Next Mater. 7 (2025) 100370.
[110] S.K. Bhar, et al., Photocatalytic degradation of organic dye on porous iron sulfide film surface, J. Colloid Interface Sci. 393 (2013) 286–290.
[111] G.S. Sree, et al., Deterioration of cadmium and pathogens from contaminated water using hydrothermally prepared NiO-ZnO-RGO composite, J. Mater. Res. Technol. 10 (2021) 976–987.
[112] M. Thanavel, et al., Synergistic effect of biological and advanced oxidation process treatment in the biodegradation of Remazol yellow RR dye, Sci. Rep. 10 (1) (2020) 20234.
[113] A. Meher, et al., Synthesis of zinc oxide/bismuth oxide nanocomposite photocatalyst for visible light-assisted degradation of synthetic dyes and antibacterial application, Environ. Sci. Pollut. Res. (2025) 1–25.
[114] F. Xu, et al., Synthesis of ZnO/CdS hierarchical heterostructure with enhanced photocatalytic efficiency under nature sunlight, CrystEngComm 14 (10) (2012) 3615–3622.
[115] C. Han, et al., Improving the photocatalytic activity and anti-photocorrosion of semiconductor ZnO by coupling with versatile carbon, Phys. Chem. Chem. Phys. 16 (32) (2014) 16891–16903.
[116] V.H.-T. Thi, B.-K. Lee, Effective photocatalytic degradation of paracetamol using La-doped ZnO photocatalyst under visible light irradiation, Mater. Res. Bull. 96 (2017) 171–182.
[117] S. Sohrabnezhad, A. Seifi, The green synthesis of ag/ZnO in montmorillonite with enhanced photocatalytic activity, Appl. Surf. Sci. 386 (2016) 33–40.
[118] G.T. Rao, et al., Synthesis and characterization of VO2+ doped ZnO–CdS composite nanopowder, J. Mol. Struct. 1081 (2015) 254–259.
[119] S.-W. Cao, et al., Preparation and photocatalytic property of α-Fe2O3 hollow core/shell hierarchical nanostructures, J. Phys. Chem. Solid 71 (12) (2010) 1680–1683.
[120] A. Suguna, et al., A detailed investigation on the structural, optical, and photocatalytic properties of ZnO@ ZnS core–shell nanostructures, J. Mater. Sci. Mater. Electron. 34 (23) (2023) 1655.
[121] S. Jangra, et al., MXene decorated ZnO-tetrapod for efficient degradation of methyl Orange, methylene blue, and rhodamine B dyes, Mater. Sci. Eng.: B 311 (2025) 117832.
[122] X. Jin, et al., Solid-state synthesis of ZnO/ZnS photocatalyst with efficient organic pollutant degradation performance, Catalysts 12 (9) (2022) 981.
[123] H. Salaheldin, A. Aboelnga, A. Elsayed, Mycosynthesis of zinc sulfide/zinc oxide nanocomposite using fusarium oxysporum for catalytic degradation of methylene blue dye, antimicrobial, and anticancer activities, Sci. Rep. 14 (1) (2024) 32165.
[124] U.M. Bayram, C.I.D. Özer, E. Yilmaz, Comparison of photocatalytic and adsorption properties of ZnS@ ZnO, CdS@ ZnO, and PbS@ ZnO nanocomposites to select the best material for the bifunctional removal of methylene blue, ACS Omega 10 (10) (2025) 9986–10003.
[125] S. Yousaf, et al., Solar light irradiated photocatalytic activity of ZnO–NiO/rGO nanocatalyst, J. Mater. Res. Technol. 12 (2021) 999–1009.
[126] L. Song, et al., Synthesis of CuS microspheres from constituent elements and its photocatalytic application, Mater. Res. Innov. 21 (4) (2017) 232–236.
[127] Y. Yulizar, D.O.B. Apriandanu, F.L. Hakim, Two-phase synthesis in n-hexane–water, characterization, and photocatalytic activity of ZnO/Bi 2 Sn 2 O 7 nanocomposite, JOM 73 (2021) 441–449.

[128] S. Anbazhagi, et al., Synthesis, characterization, in silico, and in vitro studies of CuS–ZnO nanocomposite using mushroom extract, Hybrid Adv. 8 (2025) 100390.
[129] A.Q. Malik, et al., Synthesis, characterization, photocatalytic effect of CuS-ZnO nanocomposite on photodegradation of Congo red and phenol pollutant, Inorg. Chem. Commun. 143 (2022) 109797.
[130] I. Zgura, et al., Wet chemical synthesis of ZnO-CdS composites and their photocatalytic activity, Mater. Res. Bull. 99 (2018) 174–181.
[131] H.M. Naeem, et al., HF-based surface modification for enhanced photobiological and photochemical performance of ZnO and ZnO/CdS hierarchical structures, Mater. Chem. Phys. 252 (2020) 123190.
[132] S. Yuvaraj, et al., Hydrothermal synthesis of ZnO–CdS nanocomposites: structural, optical and electrical behavior, Ceram. Int. 46 (1) (2020) 391–402.
[133] J. Nayak, et al., CdS–ZnO composite nanorods: synthesis, characterization and application for photocatalytic degradation of 3, 4-dihydroxy benzoic acid, Appl. Surf. Sci. 254 (22) (2008) 7215–7218.
[134] X. Zhang, et al., Photocatalytic activity of 3D flower-like MoS2 hemispheres, Mater. Res. Bull. 100 (2018) 249–253.
[135] S. Liu, et al., Synthesis and adsorption/photocatalysis performance of pyrite FeS2, Appl. Surf. Sci. 268 (2013) 213–217.
[136] D. Mohammadi Azar, et al., Preparation of FeS2/ZnO nanocomposites for efficient photocatalytic degradation of organic pollution from water: optical, structural, and optimisation studies, Int. J. Environ. Anal. Chem. (2021) 1–13.
[137] A. Makama, et al., Influence of parameters and radical scavengers on the visible-light-induced degradation of ciprofloxacin in ZnO/SnS2 nanocomposite suspension: identification of transformation products, Chemosphere 253 (2020) 126689.
[138] A. Makama, et al., Microwave-assisted synthesis of porous ZnO/SnS_2 heterojunction and its enhanced photoactivity for water purification, J. Nanomater. 2015 (1) (2015) 108297.
[139] Y.-N. Luo, et al., Excellent photocatalytic performance from NiS decorated TiO2 nanoflowers with exposed {001} facets, Mater. Res. Bull. 130 (2020) 110945.
[140] G. Li, et al., Graphene-bridged WO3/MoS2 Z-scheme photocatalyst for enhanced photodegradation under visible light irradiation, Mater. Chem. Phys. 246 (2020) 122827.
[141] X. Meng, et al., Efficient photocatalytic CO2 reduction in all-inorganic aqueous environment: cooperation between reaction medium and cd (II) modified colloidal ZnS, Nano Energy 34 (2017) 524–532.
[142] Y. Zhou, et al., An efficient method to enhance the stability of sulphide semiconductor photocatalysts: a case study of N-doped ZnS, Phys. Chem. Chem. Phys. 17 (3) (2015) 1870–1876.
[143] M.E. Aguirre, et al., Cu2O/TiO2 heterostructures for CO2 reduction through a direct Z-scheme: protecting Cu2O from photocorrosion, Appl. Catal. Environ. 217 (2017) 485–493.
[144] J. Murillo-Sierra, et al., Construction of direct Z-scheme WO3/ZnS heterojunction to enhance the photocatalytic degradation of tetracycline antibiotic, J. Environ. Chem. Eng. 9 (2) (2021) 105111.
[145] S.G.K. Patro, A. Hota, A.O. Salau, Photo-catalytic reduction of destructive U (VI) from uranium-defiled wastewater: an overview, Water Air Soil Pollut. 235 (5) (2024) 279.
[146] Y. Ye, et al., Removal and recovery of aqueous U (VI) by heterogeneous photocatalysis: progress and challenges, Chem. Eng. J. 450 (2022) 138317.
[147] M. Qiu, et al., The photocatalytic reduction of U (VI) into U (IV) by ZIF-8/g-C3N4 composites at visible light, Environ. Res. 196 (2021) 110349.
[148] T. Di, et al., Review on metal sulphide-based Z-scheme photocatalysts, ChemCatChem 11 (5) (2019) 1394–1411.
[149] J.-M. Bonmatin, et al., Residues of neonicotinoids in soil, water and people's hair: a case study from three agricultural regions of the Philippines, Sci. Total Environ. 757 (2021) 143822.
[150] Yousefia, F. and A. Nezamzadeh-Ejhieha, *Photodegradation of phenazopyridine in an aqueous solution by CdS-WO.*
[151] M.G. Peleyeju, E.L. Viljoen, WO3-based catalysts for photocatalytic and photoelectrocatalytic removal of organic pollutants from water–a review, J Water Process Eng 40 (2021) 101930.
[152] A.A. Shah, A.D. Chandio, A.A. Sheikh, Boron doped ZnO nanostructures for photo degradation of methylene blue, methyl orange and rhodamine B, J. Nanosci. Nanotechnol. 21 (4) (2021) 2483–2494.
[153] M. Guo, et al., Rational design of molybdenum sulfide/tungsten oxide solar absorber with enhanced photocatalytic degradation toward dye wastewater purification, J. Colloid Interface Sci. 631 (2023) 33–43.
[154] S. Singla, S. Sharma, S. Basu, MoS2/WO3 heterojunction with the intensified photocatalytic performance for decomposition of organic pollutants under the broad array of solar light, J. Clean. Prod. 324 (2021) 129290.
[155] L.A. Etshindo, et al., SnO2-TiO2 materials for photocatalytic degradation of cationic dye under UV and visible light and a chitosan composite film investigation, Catal. Today 444 (2025) 114995.
[156] J. Tian, et al., Recent progress in design, synthesis, and applications of one-dimensional TiO 2 nanostructured surface heterostructures: a review, Chem. Soc. Rev. 43 (20) (2014) 6920–6937.
[157] J. Zhang, et al., New understanding on the different photocatalytic activity of wurtzite and zinc-blende CdS, Appl. Catal. Environ. 192 (2016) 101–107.
[158] F. Tian, et al., Pouous TiO2 nanofibers decorated CdS nanoparticles by SILAR method for enhanced visible-light-driven photocatalytic activity, Appl. Surf. Sci. 391 (2017) 295–302.
[159] X. Li, et al., The synthesis of CdS/TiO2 hetero-nanofibers with enhanced visible photocatalytic activity, J. Colloid Interface Sci. 452 (2015) 89–97.
[160] A. Franco, et al., Photocatalytic decolorization of methylene blue in the presence of TiO2/ZnS nanocomposites, J. Hazard. Mater. 161 (1) (2009) 545–550.
[161] V. Štengl, et al., Visible-light photocatalytic activity of TiO2/ZnS nanocomposites prepared by homogeneous hydrolysis, Microporous Mesoporous Mater. 110 (2–3) (2008) 370–378.
[162] M. Li, et al., Tuning piezoelectric driven photocatalysis by TiO2/ZnS heterojunction for mineral processing wastewater degradation, J Water Process Eng 64 (2024) 105727.
[163] Z. Long, et al., Preparation and application of BiOBr-Bi2S3 heterojunctions for efficient photocatalytic removal of Cr (VI), J. Hazard. Mater. 407 (2021) 124394.
[164] M. Arumugam, et al., Solvent-mediated synthesis of BiOI with a tunable surface structure for effective visible light active photocatalytic removal of Cr (VI) from wastewater, Environ. Res. 197 (2021) 111080.
[165] D. Zeng, et al., Theoretical and experimental research of novel fluorine doped hierarchical Sn3O4 microspheres with excellent photocatalytic performance for removal of Cr (VI) and organic pollutants, Chem. Eng. J. 391 (2020) 123607.
[166] J. Ma, et al., Fabrication of core–shell TiO2@CuS nanocomposite via a bifunctional linker-assisted synthesis and its photocatalytic performance, J. Mater. Sci. 54 (4) (2019) 2928–2939.
[167] Y. Jiang, et al., Construction of immobilized CuS/TiO2 nanobelts heterojunction photocatalyst for photocatalytic degradation of enrofloxacin: synthesis, characterization, influencing factors and mechanism insight, J. Chem. Technol. Biotechnol. 94 (7) (2019) 2219–2228.
[168] G.H. Priya, et al., Fabrication and characterization of TiO2/CuS nanocomposites (Cu= 0.25, 0.50, and 0.75 M) utilized for the photocatalytic degradation of crystal violet dye, J. Mater. Res. 37 (23) (2022) 4182–4199.
[169] C. Wang, et al., Controlled formation of TiO2/MoS2 core–shell heterostructures with enhanced visible-light photocatalytic activities, Part. Part. Syst. Charact. 33 (4) (2016) 221–227.
[170] M. Govinda Raj, et al., TiO2 nanorod decorated with MoS2 nanospheres: an efficient dual-functional photocatalyst for antibiotic degradation and hydrogen production, Chemosphere 357 (2024) 142033.
[171] Y.C. Zhang, J. Li, H.Y. Xu, One-step in situ solvothermal synthesis of SnS2/TiO2 nanocomposites with high performance in visible light-driven photocatalytic reduction of aqueous Cr(VI), Appl. Catal. Environ. 123-124 (2012) 18–26.
[172] J. Rashid, et al., Stabilized fabrication of anatase-TiO 2/FeS2 (pyrite) semiconductor composite nanocrystals for enhanced solar light-mediated photocatalytic degradation of methylene blue, RSC Adv. 8 (22) (2018) 11935–11945.
[173] K. Kumari, et al., Efficient visible-light photocatalysis using Fe-doped SnO2/chitosan composite for organic pollutant degradation: mechanisms, reusability, and sustainability, J. Inorg. Organomet. Polym. Mater. (2025) 1–24.
[174] E.E. El-Katori, et al., Impact of CdS/SnO2 heterostructured nanoparticle as visible light active photocatalyst for the removal methylene blue dye, J Photochem Photobiol A Chem 392 (2020) 112403.
[175] L. Zhang, et al., One-step in situ synthesis of CdS/SnO2 heterostructure with excellent photocatalytic performance for Cr(VI) reduction and tetracycline degradation, Chem. Eng. J. 352 (2018) 863–875.
[176] H. Du, et al., Fabrication of recoverable Bi2O2S/Bi5O7I/ZA hydrogel beads for enhanced photocatalytic Hg0 removal in the presence of H2O2, Sep. Purif. Technol. 359 (2025) 130597.
[177] M.F. Sanad, et al., The controlled synthesis and DFT investigation of novel (0D)–(3D) ZnS/SiO 2 heterostructures for photocatalytic applications, RSC Adv. 11 (36) (2021) 22352–22364.
[178] D. Dissanayake, et al., Facile and low-cost synthesis of pure hematite (α-Fe 2 O 3) nanoparticles from naturally occurring laterites and their superior adsorption capability towards acid-dyes, RSC Adv. 9 (37) (2019) 21249–21257.
[179] H. Zhang, et al., Preparation of magnetic α-Fe2O3/ZnFe2O4@ Ti3C2 MXene with excellent photocatalytic performance, Ceram. Int. 46 (1) (2020) 81–88.
[180] G. Khabiri, et al., A novel α-Fe2O3@MoS2QDs heterostructure for enhanced visible-light photocatalytic performance using ultrasonication approach, Ceram. Int. 46 (11, Part B) (2020) 19600–19608.
[181] M.R. Shariati, A. Samadi-Maybodi, A.H. Colagar, Exploration of charge carrier delocalization in the iron oxide/CdS type-II heterojunction band alignment for enhanced solar-driven photocatalytic and antibacterial applications, J. Hazard. Mater. 366 (2019) 475–481.
[182] Y.C. Zhang, et al., One-step hydrothermal synthesis of high-performance visible-light-driven SnS2/SnO2 nanoheterojunction photocatalyst for the reduction of aqueous Cr(VI), Appl. Catal. Environ. 144 (2014) 730–738.
[183] C. Venkata Reddy, et al., Synthesis of CdO/ZnS heterojunction for photodegradation of organic dye molecules, Appl. Phys. A 123 (2017) 1–12.
[184] M. Parvaz, et al., Synthesis, characterization, and photocatalytic properties of CuO-TiS2 nanocomposite, Mater Res Express 6 (12) (2019) 125054.
[185] E.O. Ichipi, et al., A comparative study of metal-sulphide/ZnO for visible-light-induced photocatalysis and the six-flux photon absorption model of an external lamp photoreactor, J. Environ. Chem. Eng. 12 (5) (2024) 113355.
[186] I. Zgura, et al., Wet chemical synthesis of ZnO-CdS composites and their photocatalytic activity, Mater. Res. Bull. 99 (2018) 174–181.
[187] A. Alsulmi, et al., Rational design of magnetic recyclable S-scheme FeS2/TiO2 heterojunction for photocatalytic degradation of rhodamine B dye under broad solar spectrum, J. Inorg. Organomet. Polym. Mater. 34 (4) (2024) 1628–1642.
[188] X. Ning, G. Lu, Photocorrosion inhibition of CdS-based catalysts for photocatalytic overall water splitting, Nanoscale 12 (3) (2020) 1213–1223.
[189] L. Meng, L. Li, Recent research progress on operational stability of metal oxide/sulfide photoanodes in photoelectrochemical cells, Nano Res. Energy 1 (2) (2022) p. e9120020-e9120020.

[190] X. Yi, et al., Analysis of heavy metal pollution sources caused by sulfide minerals in tunnel waste under photocatalytic oxidation conditions, Environ. Sci. Pollut. Res. 32 (18) (2025) 11550–11561.
[191] V.R. Santoyo, et al., Metal oxide-based nanoparticles for environmental remediation: drawbacks and opportunities, Period. Polytechn. Chem. Eng. 68 (3) (2024) 311–325.
[192] W. Luc, F. Jiao, Synthesis of nanoporous metals, oxides, carbides, and sulfides: beyond nanocasting, Acc. Chem. Res. 49 (7) (2016) 1351–1358.
[193] E. Kociołek-Balawejder, et al., Sulphidation of Cu 2+, CuO and Cu 2 O within the matrix of carboxylic cation exchangers–compositional, morphological and thermal properties of Cu x S containing composites, React. Chem. Eng. 10 (5) (2025) 1077–1095.
[194] G. Hussain, et al., Exploring the structural stability, electronic and thermal attributes of synthetic 2D materials and their heterostructures, Appl. Surf. Sci. 590 (2022) 153131.



Atiqa Aslam is an MPhil graduate in Chemistry with a focus on nanomaterials for environmental and energy applications. Her studies investigate the synthesis and characterization of novel advanced nanomaterials, such as metal oxides, metal sulfides, polymers, binary/ternary heterojunctions, to photocatalytically degrade pollutants and electrochemical devices, including supercapacitors. Her MPhil work was on multifunctional materials for wastewater treatment and electrode materials for energy storage. She has done scholarly work, including conference papers and presentations at national and international conferences.



Nimra Nadeem is a Research Associate on a UK-funded project focusing on the molecular distortion of pollutants from wastewater. She completed her Ph.D. Balaussa Balgabayeva[2,3], Sami Ullah Khan metal oxide metal ferrites with CFA, GCN, and GO composites) for wastewater treatment. With extensive experience in energy and environmental research, her expertise lies in advanced nanomaterials, photocatalysis, and polymeric membranes. Her research includes flexible supercapacitors, wearable sensors, energy-efficient textiles. Their research also integrates AI-driven modeling, including Gaussian Process Regression, for predictive analysis in photocatalysis and wastewater treatment. She has authored several publications in reputable journals, contributed to book chapters, and presented at national and international conferences.



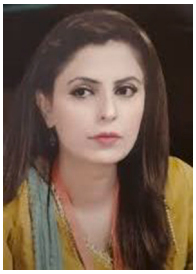
Balaussa Balgabayeva is currently pursuing her Master's degree at Al-Farabi Kazakh National University. Her research focuses on the development of energy storage technologies, particularly enhancing the energy capacity of batteries and supercapacitors using electrochemically reduced graphene oxide (ErGO). Her academic interests lie in advanced nanomaterials for energy storage, electrochemical performance optimization, and the sustainable application of graphene-based composites.



Sami Ullah Khan, PhD is a distinguished young research scientist at Paracelsus Medical University, Salzburg, Austria. His research centers on electron transfer flavoprotein (ETF) and its pivotal role in cellular energy production, with a strong focus on the electrochemical mechanisms driving these vital biological processes. Dr. Khan is an expert in understanding enzyme mechanisms, particularly the electrochemical behavior and modifications of flavin adenine dinucleotide (FAD) cofactors, which are crucial for electron transfer reactions. Dr. Khan holds a PhD from the Technical University of Graz, Austria, where his dissertation explored flavin cofactor modifications in human electron transfer flavoprotein. His groundbreaking work includes the discovery of 8C-FAD, a novel cofactor in human electron transfer flavoprotein, significantly advancing the understanding of biological electrochemistry. His research portfolio encompasses a range of projects from advanced in-silico molecular modeling of electron transfer pathways to the development of pharmaceutical formulations and analytical techniques. Dr. Khan's expertise is further demonstrated through his roles as a thesis supervisor and instructor in Pharmaceutical Technology, Bioanalytical Techniques, Molecular Diagnostics, and Data Analysis. He is a highly awarded academic, recognized with the "Best Teacher Award" and "Dean's Outstanding Researcher" accolades, alongside multiple prestigious fellowships.



Qamar Abbas, PhD has led a number of research projects at Graz University of Technology, Graz, Austria including ECO-CAPs (funded by the FFG) and Lise Meitner Project (funded by the FWF). His research focused on harnessing iodine electrochemical properties in fast energy storage devices such as hybrid supercapacitors and batteries. Q. Abbas is an expert on nanoporous carbon materials, iodine electrochemistry and eco-friendly electrolytes for fast electrochemical energy storage. Currently, he leads NCN funded project at Poznan University of Technology, Poland. He has published over 80 peer-reviewed articles with a total citation over 3000.



Saima Noreen, PhD is a distinguished physical chemist currently serving in the Department of Chemistry at the University of Agriculture, Faisalabad, where she joined on September 8, 2015. With a strong research background spanning polymer chemistry, wastewater management, nanotechnology, computational chemistry, and materials science, Dr. Noreen has made significant contributions to the advancement of interdisciplinary chemical sciences. Her work in materials science focuses on the design and development of functional materials for environmental and energy-related applications, including nanomaterials for pollutant removal and catalytic systems for sustainable technologies. Dr. Noreen is also a passionate researcher of green chemistry, emphasizing the development of eco-friendly processes and materials to minimize environmental impact and support a circular economy. She has an impressive academic record, with 129 peer-reviewed publications, an h-index of 36, an i10-index of 63, and over 5122 citations, reflecting the high impact and recognition of her work in the scientific community. Her research continues to address critical global challenges through innovative solutions in environmental remediation, sustainable materials, and green chemical processes.



Muhammad Zahid, PhD is a Professor of Chemistry at the University of Agriculture Faisalabad (UAF) Pakistan. His research interests include the synthesis of advanced nanomaterials such as graphene based functional materials, carbon quantum dots, semiconductor nanoparticles, etc., and their applications in environmental remediation as well as in energy materials. He is actively involved in the synthesis of heterojunctions, metal doping, nanocomposites, polymer composites etc. along with their promising applications in energy, environment and sensors. Dr. Zahid has published 04 books, 29 book chapters and more than 160 peer-reviewed journal articles with a citation score of above 5000. He has steered several research projects for developing new materials with their applications in environment, energy, sensors, etc.



Zhazira Supiyeva, PhD is an Associate Professor at Al-Farabi Kazakh National University, Faculty of Chemistry and Chemical Technology. Her research focuses on nanomaterials and nanotechnologies in the field of chemical sciences. She has received several honors, including being recognized as The Best Young Scientist of KazNU and receiving the JESH scholarship from the Austrian Academy of Sciences. Her area of expertise includes the study of electrochemical processes occurring on novel carbon materials applicable in supercapacitors, as well as the development of scientific, technological, and innovative support for industries using electrochemical methods for extraction, analysis, and production of new substances and materials. Currently, she leads research projects funded by the Committee of Science of the Ministry of Science and Higher Education of the Republic of Kazakhstan. She has published 21 high-impact papers (H-index: 7) in journals such as Current Opinion in Electrochemistry and Materials Science and Engineering: R: Reports.